RI 8350

Bureau of Mines Report of Investigations/1979

# Corrosion Studies in Brines of the Salton Sea Geothermal Field



UNITED STATES DEPARTMENT OF THE INTERIOR

## DISCLAIMER

Report of Investigations 8350

# Corrosion Studies in Brines of the Salton Sea Geothermal Field

By J. P. Carter, F. X. McCawley, S. D. Cramer, and P. B. Needham, Jr.




UNITED STATES DEPARTMENT OF THE INTERIOR
Cecil D. Andrus, Secretary

BUREAU OF MINES
Roger A. Markle, Director

This publication has been cataloged as follows:

Corrosion studies in brines of the Salton Sea geothermal field / by J. P. Carter ... [et al.] [Washington] : U.S. Dept. of the Interior, Bureau of Mines, 1979.

35 p. : ill., diagrs. ; 27 cm. (Report of investigations • Bureau of Mines ; 8350)

Bibliography: p. 35.

1. Geothermal resources • Salton Sea region. 2. Salt. 3. Corrosion and anticorrosives. I. Carter, John P. II. United States. Bureau of Mines. III. Series: United States. Bureau of Mines. Report of investigations • Bureau of Mines ; 8350.

TN23.U7 no. 8350 622.06173

U.S. Dept. of the Int. Library

CONTENTS



ILLUSTRATIONS

ILLUSTRATIONS--Continued



TABLES

TABLES--Continued

Bureau of Mines
Report of Investigations 8350

# CORROSION STUDIES IN BRINES OF THE SALTON SEA GEOTHERMAL FIELD

by

J. P. Carter, F. X. McCawley, S. D. Cramer,
and P. B. Needham, Jr.

---

## ERRATA

On page 24, please replace table 12 with the corrected version.

NOTE: Page 24 has been reproduced on gummed paper for your convenience. Please moisten and place in position.

# CORROSION STUDIES IN BRINES OF THE SALTON SEA GEOTHERMAL FIELD

by

J. P. Carter,[1] F. X. McCawley,[2] S. D. Cramer,[3]
and P. B. Needham, Jr.[4]

## ABSTRACT

Toward the goal of maximizing minerals and metals recovery from domestic resources, the Bureau of Mines, U.S. Department of the Interior, has conducted in situ corrosion studies at the Salton Sea Known Geothermal Resources Area (KGRA) in the Imperial Valley, Calif., to evaluate and characterize materials of construction for geothermal resources recovery plants. General-, pitting, and crevice-corrosion characteristics of 13 commercially available alloys were investigated for periods of 15 and 30 days in seven process environments expected to be found in typical geothermal resources plants.

Stainless steel alloy 29-4, Inconel 625, and the Hastelloys G, S, and C-276 were the most resistant to general corrosion, did not pit, and exhibited little susceptibility to crevice corrosion. Stainless steel alloys 430, E-Brite 26-1, and 6X had low general corrosion rates, but pitted and were susceptible to crevice corrosion. Stainless steel alloy 316 L had a low corrosion rate, but corroded intergranularly, pitted, and was susceptible to crevice corrosion and to stress-corrosion cracking. Titanium-1.5 nickel and TiCode-12 had low corrosion rates, did not pit, and were not susceptible to crevice corrosion. Carbon and 4130 steels had high corrosion rates, pitted, and had high susceptibilities to crevice corrosion. The major scale-forming mineral on the corrosion samples in most of the process environments studied was galena mixed with lesser amounts of other minerals.

## INTRODUCTION

The Imperial Valley of California is one of the major liquid-dominated geothermal regions in the United States. Within this valley are several large and distinct Known Geothermal Resources Areas (KGRA) that contain substantial

[1]Research chemist, Avondale Metallurgy Research Center, Bureau of Mines, Avondale, Md.
[2]Metallurgist, Avondale Metallurgy Research Center, Bureau of Mines, Avondale, Md.
[3]Chemical engineer, Avondale, Metallurgy Research Center, Bureau of Mines, Avondale, Md.
[4]Research physicist, Division of Metallurgy, Bureau of Mines, Washington, D.C.

quantities of dissolved, potentially recoverable metals and minerals. One such area, the Salton Sea KGRA, contains brines that not only have a high mineral content, up to 30 pct total dissolved solids (TDS) but, coupled with high temperatures, up to 350° C, they are among the most corrosive naturally occurring fluids. For this reason, recovery of these geobrine mineral resources will depend to a large measure upon materials that will withstand these severe environments.

In 1974, the Bureau of Mines undertook an extensive program of laboratory and field research and testing to identify the optimum materials of construction for potential geothermal resource recovery plants. To meet the objectives of this effort, the Bureau's Avondale (Md.) Metallurgy Research Center has conducted extensive laboratory corrosion and thermodynamic studies in brines (4, 6),[5] in addition to materials research and testing in the field.

The purpose of the field research and testing was to determine (1) the in situ corrosion properties of commercially available metals and alloys (5, 7), (2) the chemistry of flowing geothermal brines, and (3) scale deposition kinetics (1).

Two series of in situ corrosion tests were conducted in high-salinity, high-enthalpy brine from the Magmamax No. 1 geothermal well located in the Salton Sea KGRA (fig. 1). The first of these series was conducted in 1974 for 500 hours using brine and steam from the second-stage steam separator operated by the San Diego Gas & Electric Co. (SDG&E). The materials selection for this test series was based on the results of the initial laboratory corrosion measurements (4). The second series, conducted in 1976-77, consisted of two 15-day and one 30-day test of 13 alloys in seven process streams expected to be typical of geothermal resources recovery plants. Materials selection for the second test series was based on the earlier laboratory work, unreported corrosion results from tests made during 1975 in the low-salinity, medium-enthalpy brine from the East Mesa KGRA in the Imperial Valley, and the results from the 1974 test series. Reported here are the results of the two corrosion test series conducted at the Salton Sea KGRA, brine and steam chemistries, and characterization of mineral scales and deposits which formed in the seven process streams. Material failures on process equipment which occurred during operation of the Bureau's Geothermal Test Facility are also described.

ACKNOWLEDGMENT

The authors express their gratitude for the cooperation and assistance provided by personnel of the San Diego Gas & Electric Co. at their facilities on the Salton Sea KGRA. In particular, we appreciate the discussions over the past 4 years with Harry K. Bishop, Gilbert Lombard, and David Mulliner.

[5]Underlined numbers in parentheses refer to items in the list of references at the end of this report.

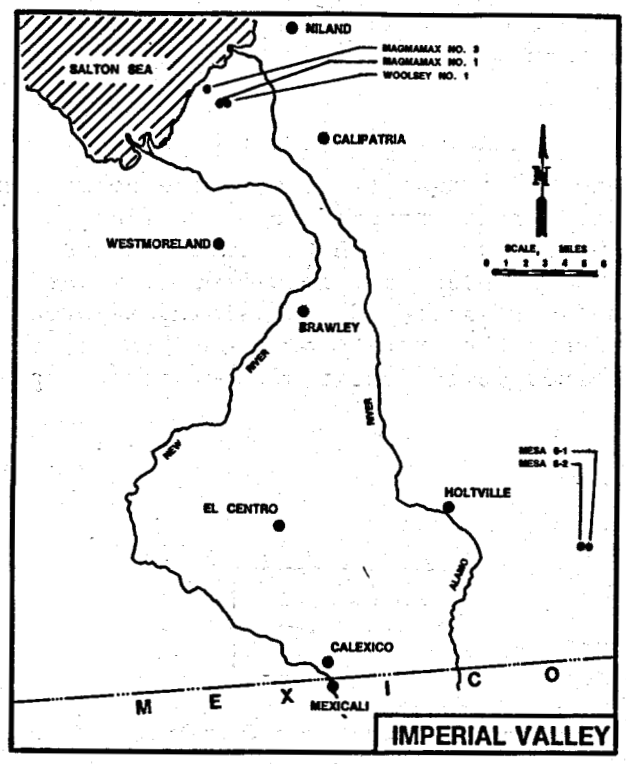


FIGURE 1. - Map of Imperial Valley of California showing select geothermal wells.

## EXPERIMENTAL

### Salton Sea KGRA--1974

The Bureau of Mines initial field geothermal corrosion test was conducted during April and May of 1974, at Magmamax well No. 1 (fig. 1) located on the high-salinity, high-enthalpy Salton Sea KGRA near Calipatria, Calif. At the test site adjacent to Magmamax No. 1 well (fig. 2), SDG&E was studying methods for separating and scrubbing steam from the geobrine produced by Magmamax No. 1 well, extracting the heat, and disposing of the spent brine. Two Bureau of Mines corrosion test packages were installed downstream from SDG&E's second-stage separator. These were placed in the concentrated brine and in the scrubbed steam lines (fig. 3). The purpose of the test was to gain first-hand experience in the field operation of a geothermal system to enable researchers to study the

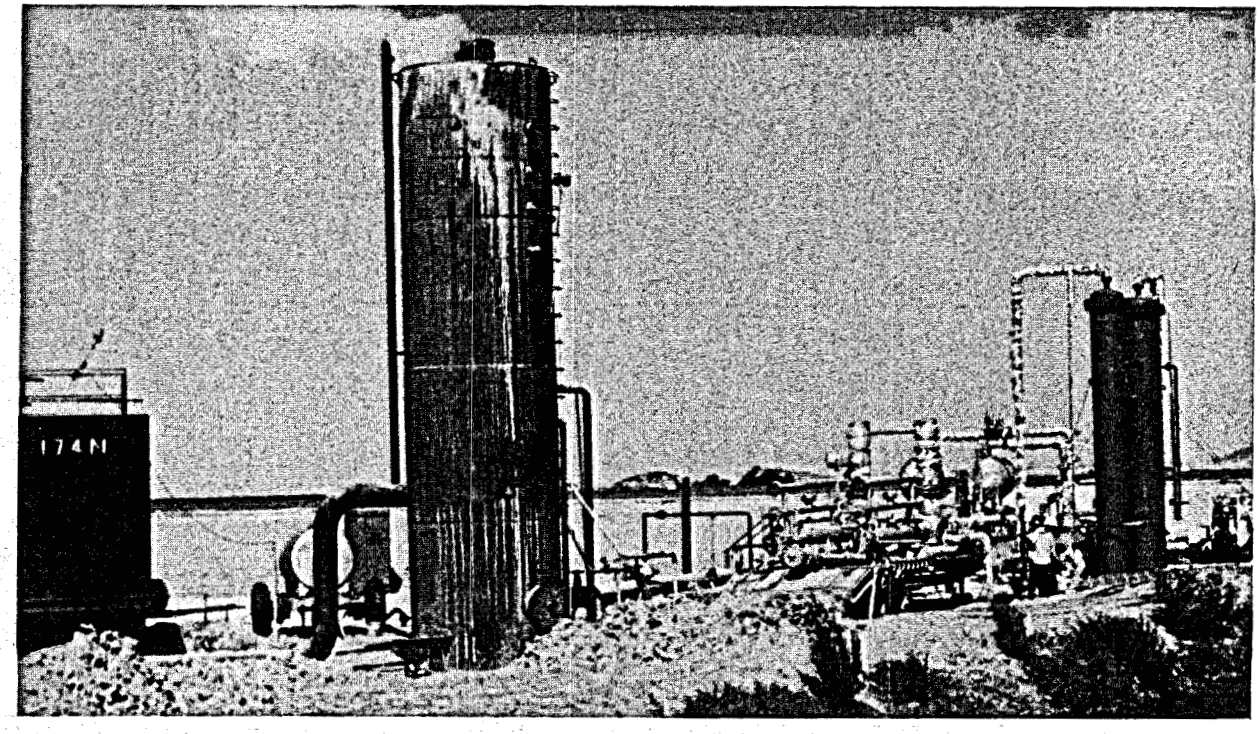


FIGURE 2. - San Diego Gas & Electric Co.'s Geothermal Loop Experimental Facility near Calipatria, Calif., 1974.

corrosion and scaling which occurs. The test consisted of 500 hours exposure of selected alloys to both environments at an average temperature of 128° C and a pressure of 50 psig.

The brine test package was constructed from eight 2-inch schedule-20 stainless steel tee's connected end-to-end by flanges (fig. 4). The corrosion test samples were mounted on stainless steel rods attached to blank flanges mounted on the side arm of each tee and were exposed both tangential to and normal to the direction of brine flow. The samples were insulated from the rods with Teflon[6] gaskets and inserts, and were fastened with stainless steel bolts. A bypass line was installed to divert the brine flow around the test package so that the samples could be examined periodically without affecting flow conditions in the SDG&E facility.

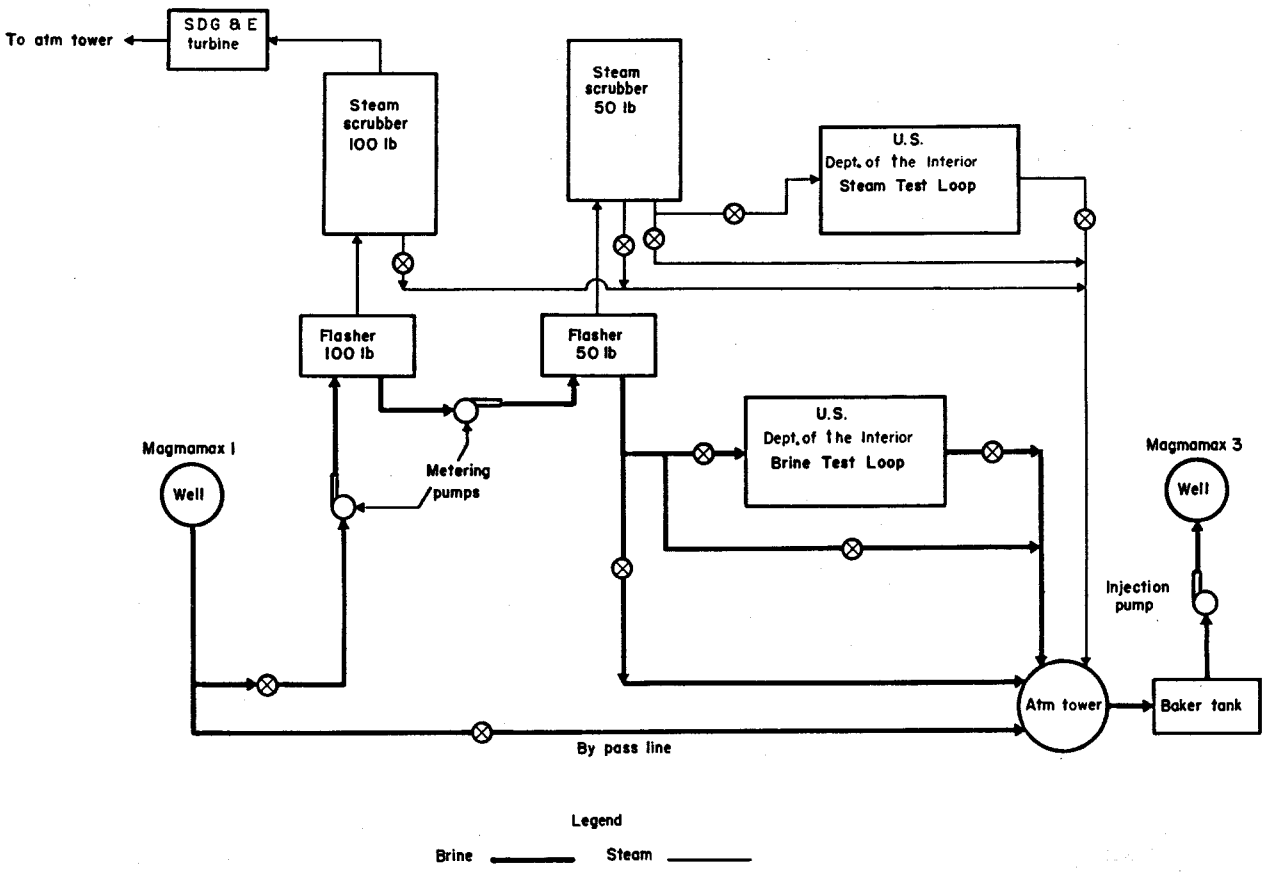


FIGURE 3. - Diagram of the SDG&E facility and the Bureau of Mines corrosion test packages, 1974.

[6]Reference to specific trade names or manufacturers is made for identification only and does not imply endorsement by the Bureau of Mines.

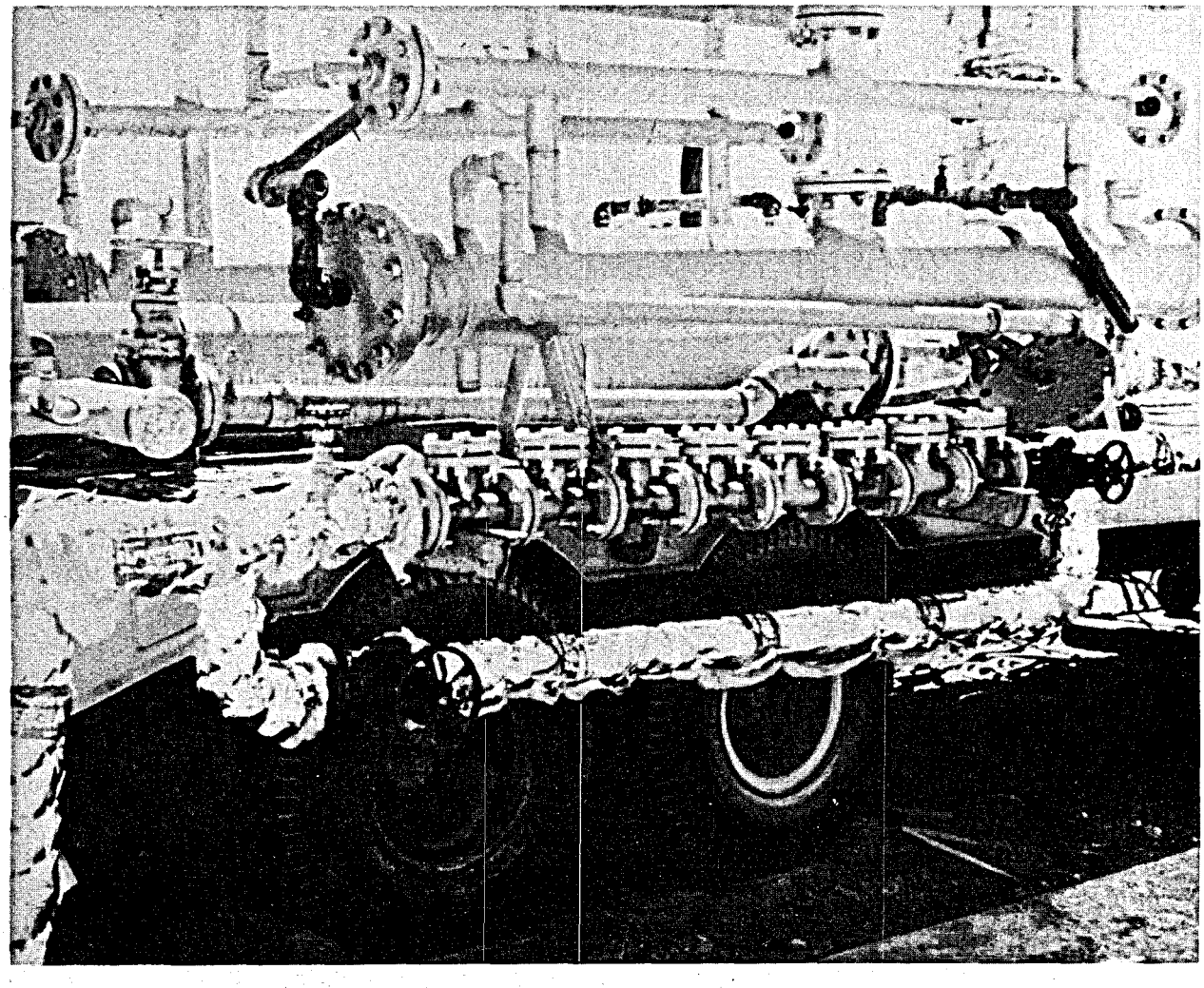

FIGURE 4. - Bureau of Mines brine corrosion test package, 1974.

The steam test package was constructed from an 8-inch-diameter, 18-inch-long carbon steel pipe (fig. 5). A steel plate was welded to one end; the other end had a removable cover. Two 3-inch-diameter, 1-inch-thick 304 stainless steel discs were welded to a 1/2-inch-diameter 304 stainless steel shaft, and this assembly was centered longitudinally in the test chamber. Samples were attached to the circular discs at an angle of 60° with respect to the plane of the discs using stainless steel bolts and were insulated from the bolts and discs by Teflon washers and inserts. Steam entered one end of the chamber and flowed across the samples.

Corrosion test samples were sheared from 1020 carbon steel, 4130 steel, Inconel 625, and Hastelloy C-276 sheet 1/16-inch thick or less. Samples exposed to the brine measured 1 by 1-1/2 inches; those exposed to the steam measured 1 by 3 inches. After shearing, the edges of all samples were ground on a 120-grit wet-belt grinder. The 1020 carbon and 4130 steel samples were pickled at 60° C in 12 vol-pct sulfuric acid containing 2.5 ml/liter (milliliter per liter) of Rodine 95 inhibitor to remove mill scale. Inconel 625 and

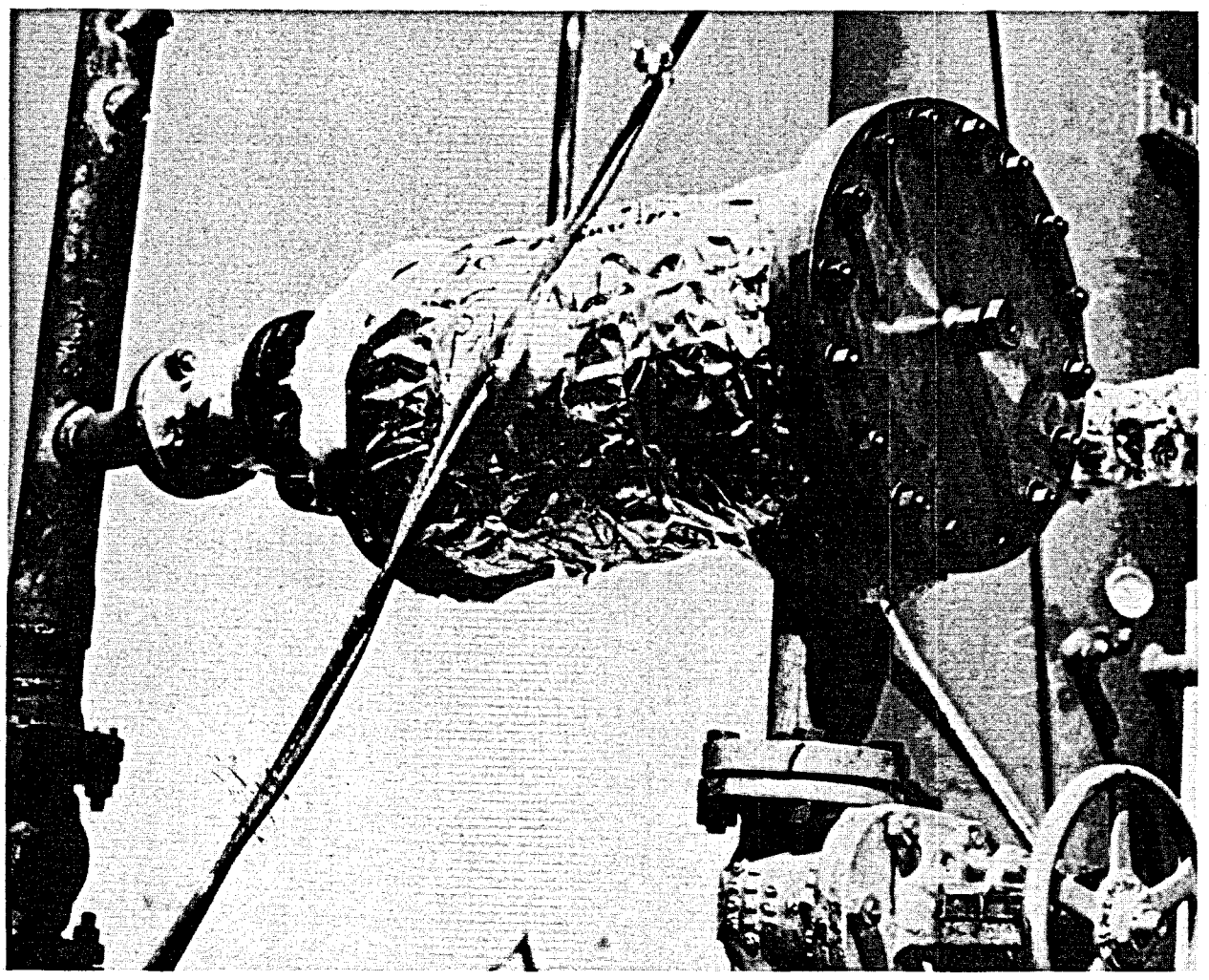

FIGURE 5. - Bureau of Mines steam corrosion test package, 1974.

Hastelloy C-276 samples were degreased in methanol and dried. Following this, treatment all samples were washed in demineralized water, dried, weighed to within ± 0.1 mg (milligram) and mounted in the test packages.

At the completion of the test, the samples were returned to the Avondale Research Center for evaluation. Adhering corrosion product and scale deposits were chipped from the corrosion samples for proton-induced X-ray emission analysis (PIXE), emission spectrographic analysis (ESA), X-ray diffraction analysis, and wet chemical analysis. Scales were examined also by scanning electron microscopy (SEM). Scale and corrosion products remaining on the samples were removed chemically. In some cases, the samples were rubbed with a rubber stopper to remove adherent products. The 1020 carbon steel and 4130 steel samples were cleaned in the inhibited 12 vol-pct sulfuric acid at 60° C. Inconel 625 and Hastelloy C-276 samples were cleaned at 60° C in 20 pct nitric acid containing, when necessary, several drops of hydrofluoric acid. After cleaning, the samples were rinsed in demineralized water, dried, and reweighed. The samples were microscopically examined and pit depths were determined.

## Salton Sea KGRA--1976-77

In May 1976, the Bureau's Geothermal Test Facility (GTF) was constructed on the Salton Sea KGRA adjacent to the SDG&E Geothermal Loop Experimental Facility. The GTF, shown in figure 6 and diagrammed in figure 7, consists of: (1) a materials testing facility (MTF) containing five in situ corrosion test packages and two steam separators mounted on a semitrailer flatbed (fig. 8); (2) two steam-scrubbing towers, plus two additional in situ corrosion test packages located in the scrubbed-steam lines; (3) three electrochemical test packages for conducting in-line electrochemical corrosion measurements; (4) two heat exchangers to condense the scrubbed steam; (5) a 30-ft-tall atmospheric pressure flashing tower into which the high-pressure spent brines from the MTF are released; (6) two 27,000-gallon Baker storage tanks for the hot spent brines from the atmospheric pressure flashing tower, (7) 320 ft of 2-inch-diameter heat-exchanger pipe in one of the storage tanks to cool the spent brines to 80° C; (8) a diesel-powered pump to inject the cooled, spent brines into Magmamax No. 3 well; (9) 21 pressure-regulator and manual flow-control valves; (10) a systems control van; (11) a 332,000-gallon cooling-water pond to supply water to the storage tank heat exchangers and to the steam condensers; and (12) a 60-ft mobile chemistry laboratory for conducting chemical analyses of the brine and the steam. A chemistry line was installed to study the effect of piping configuration and pressure drop on the chemistry of the flowing brine. A bypass line was installed around the MTF to allow the well to flow during startup, and during repairs and changing of samples in the corrosion test packages. Input brine to the Bureau's GTF was obtained from a

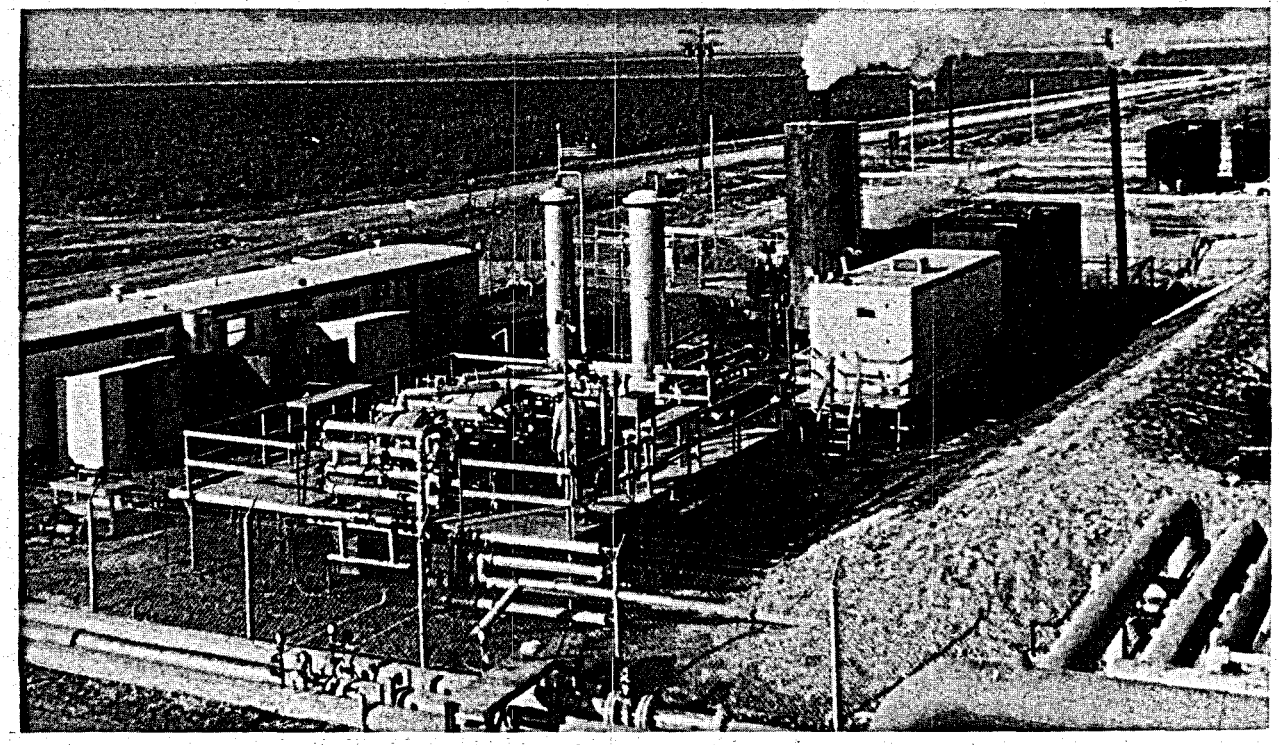

FIGURE 6. - Bureau of Mines Geothermal Test Facility near Calipatria, Calif., 1976-77.

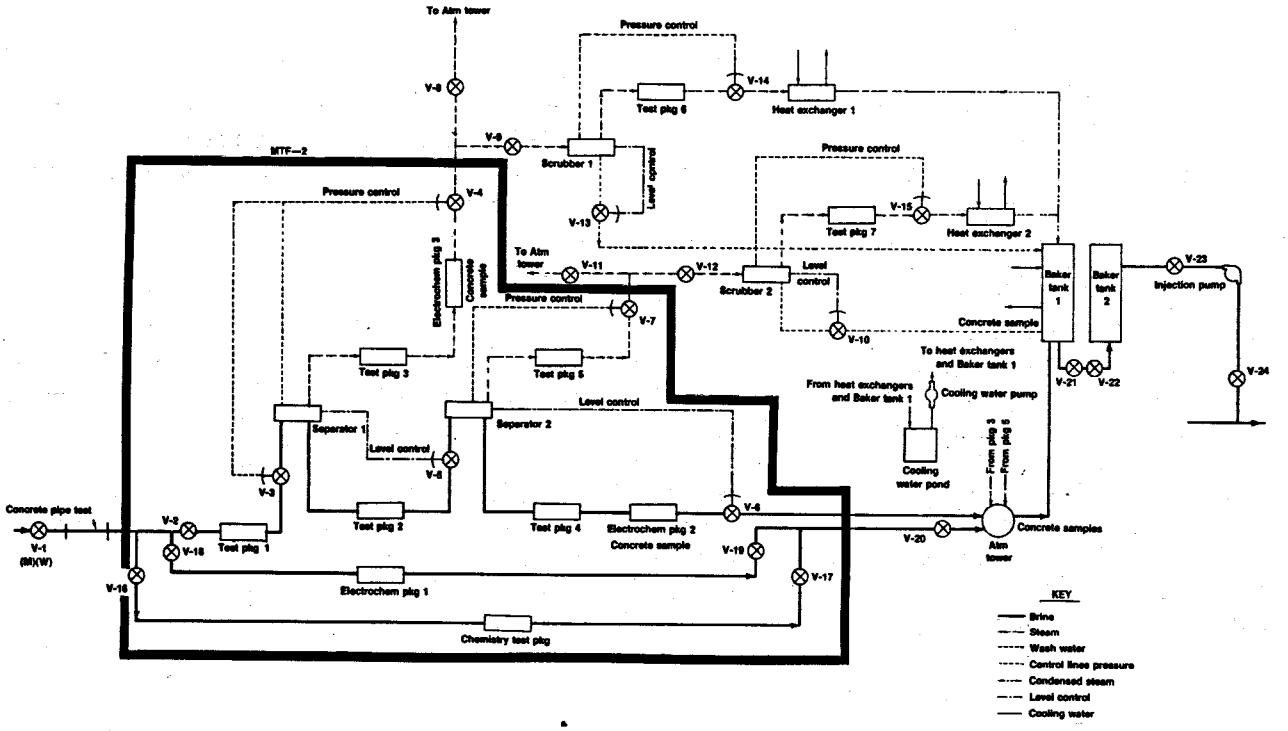


FIGURE 7. - Diagram of Bureau of Mines Geothermal Test Facility, 1976-77.

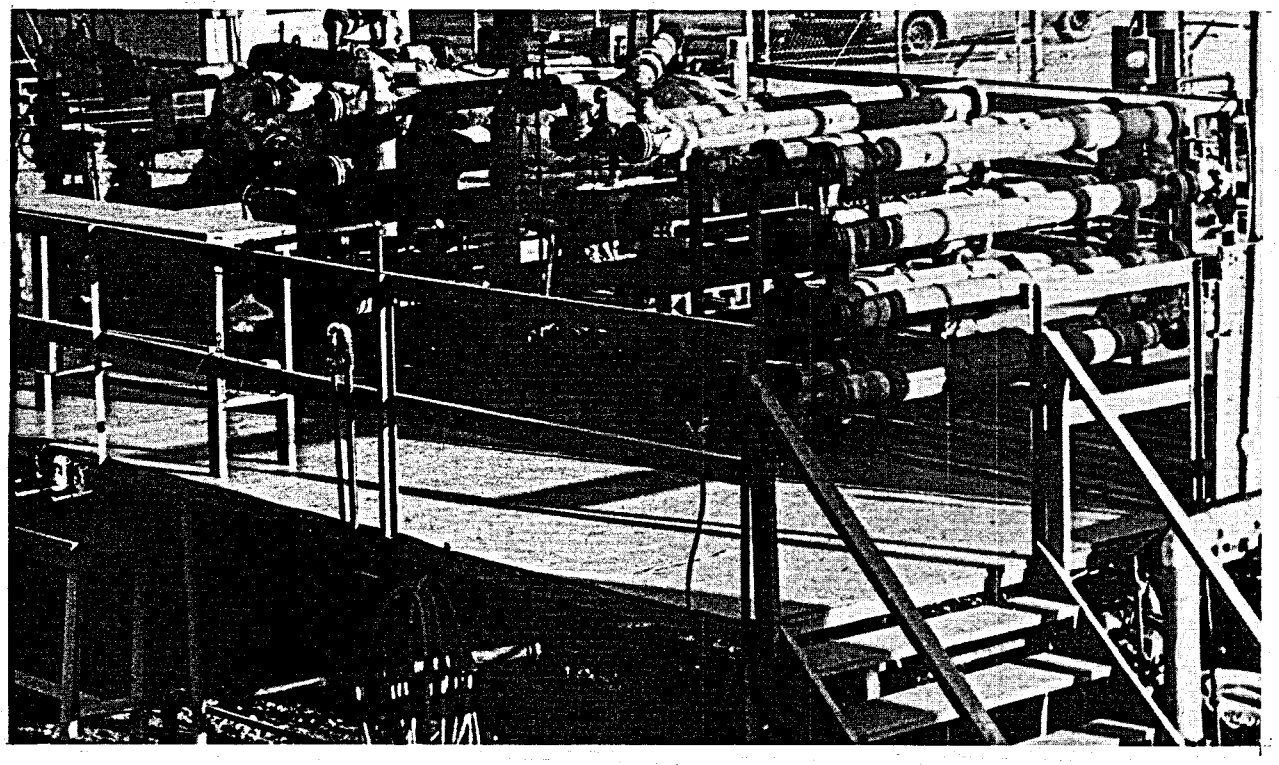

FIGURE 8. - Bureau of Mines Materials Test Facility (MTF-2) showing in situ corrosion test packages, 1976-77.

manifold welded to the 10-inch-diameter production lines from Magmamax No. 1 and Woolsey No. 1 wells which allowed brine from either well to flow into the facility.

The seven in situ corrosion test packages were constructed of 3-inch schedule-40 steel pipe, 2.9 inches inside diameter (ID), with four test sections in each test package, (fig. 9). Test sections were 8.5 feet long with blank flanges on each end. A sample support rod 5/8 by 5/8-inch square extended axially along the length of each test section. Positioning discs at the ends of the test section held the support rod in position and prevented the rod and samples from shifting during tests. Each rod held 82 weight-loss samples or 41 U-bend, stress-corrosion samples tangential to the flow. In test section A, the rod and samples were removed after each 15-day exposure, and a rod with new samples was inserted. Rods and samples in test sections B and C were removed after 30 days of operation. Test section D contained U-bend, stress-corrosion samples which were exposed for 30 days. During the 30-day test, 4,300 samples were exposed. Figure 10 shows the rods loaded with samples for the test series.

The thirteen alloys that were selected for testing are as follows:

1020 carbon steel
4130 steel
316 L stainless steel
430 stainless steel
E-Brite 26-1
Airco Vacuum Metals alloy 29-4
Allegheny Ludlum alloy 6X
Hastelloy G
Hastelloy S
Hastelloy C-276
Inconel 625
TiCode-12
Titanium-1.5 nickel

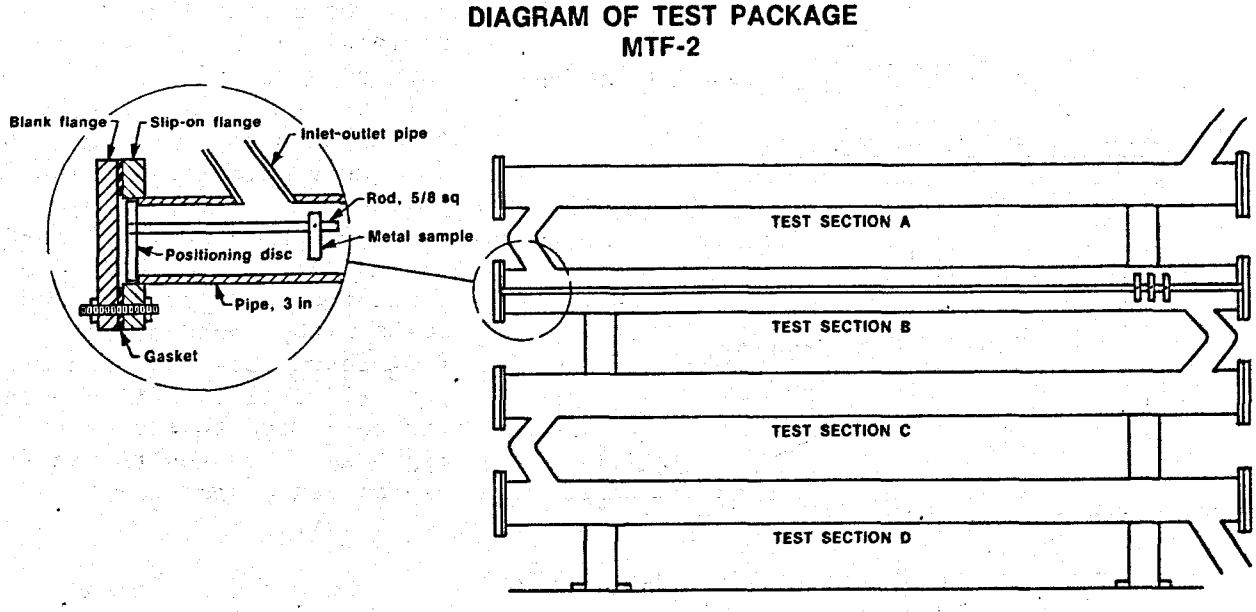


FIGURE 9. - In situ corrosion test package, 1976-77.

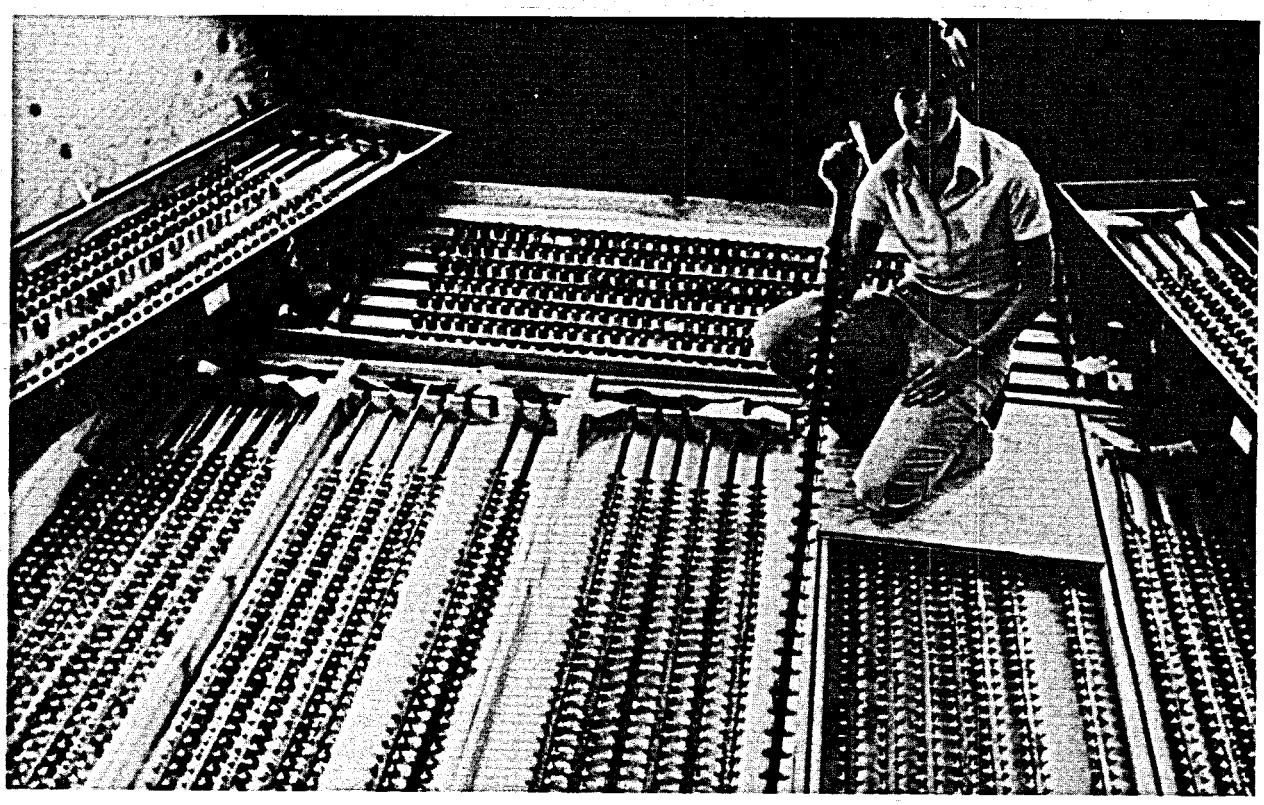

FIGURE 10. - Support rods loaded with samples for 30-day in situ corrosion test series, 1976-77.

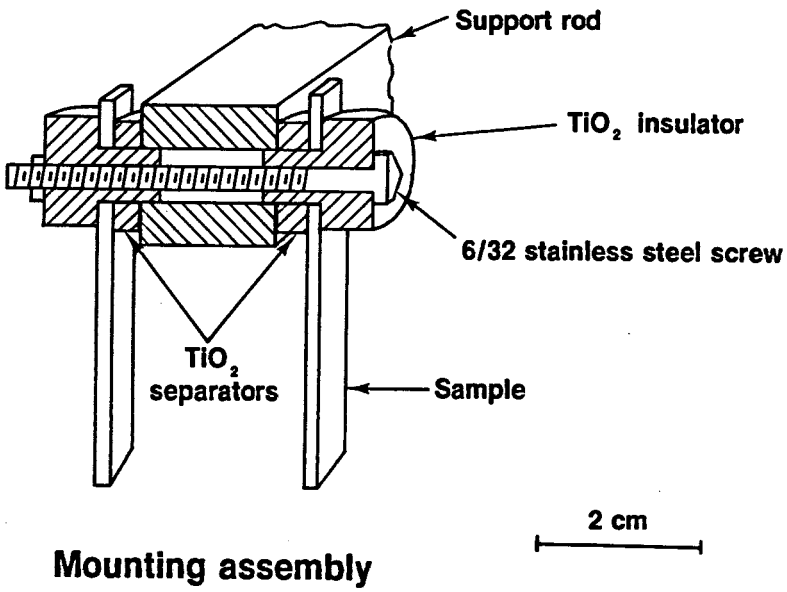


FIGURE 11. - In situ corrosion test sample mounting assembly, 1976-77.

Six to seven samples of each alloy were distributed randomly along the length of each support rod for the weight-loss tests and three to four samples were selected for the U-bend tests. The samples were mounted on the support rod with stainless steel machine bolts and insulated from the rods and bolts with nonconductive $TiO_2$ insulators and separators (fig. 11). Teflon washers were used to form a tight seal between the sample and the insulator or separator.

The seven steam and brine process streams of the GTF and their associated corrosion test packages were

labeled P1 through P7 (fig. 7) as follows: P1-Magmamax No. 1 input wellhead brine, P2-brine from the first-stage steam separator, P3-steam from the first-stage steam separator, P4-brine from the second-stage steam separator, P5-steam from the second-stage steam separator, P6-scrubbed steam from P3, and P7-scrubbed steam from P5. However, for this test the scrubbing towers were not operated and the steam entering P6 was essentially the same as from P3, and P7 was the same as that from P5.

Brine and steam velocities and the Reynolds number for each of the corrosion test packages were estimated for input-brine flow rates of 75 and 100 gpm (gallons per minute) and are presented in table 1. Mean velocities were calculated assuming that (1) the brine was in single-phase flow, (2) 10 pct of the brine flashed to steam in each steam separator, and (3) the thermodynamic data for pure $H_2O$ could be used. Average operating temperatures and pressures used in the calculations for each test package were obtained during shakedown operations of the GTF in August and September 1976. Values for the brine and steam viscosity under these conditions were estimated from the thermodynamic tables (8). The mean velocity of the brine and steam was calculated using the equation $V = Xv/A$ where V = mean velocity, fps (feet per second); v = specific volume, cfp (cubic feet per pound); X = brine or steam flow rate, pps (pounds per second); and A = cross section area of the pipe, sqf (square feet). Since the corrosion packages have an axial rod supporting the samples running the length of the pipe, the Reynolds number (2) was determined using the equation for flow through an annulus $N_{RE} = 2R(1-K)V/v\mu$, where $N_{RE}$ = Reynolds number (>2,000 = turbulent flow); v = specific volume, cfp; R = outer radius, feet; K = ratio of inner radius to outer radius; V = mean velocity, fps; and $\mu$ = viscosity, pfs (pounds per foot per second). Cross-section areas of the packages were determined using the dimensions of a 3-inch pipe with a 5/8-inch-square support centered on the pipe axis. The purpose of these calculations was to obtain an estimate of the hydrodynamic conditions prevailing in the test packages. Other assumptions, such as two-phase flow, and the use of data for concentrated brines would change the results of the calculations. However, the change would not alter the conclusions that the flow through the test packages is highly turbulent, resulting in thorough and relatively uniform exposure of the corrosion samples to the fluid, and that the surfaces of the corrosion samples are exposed to relatively high shear stresses, tending to strip away poorly adherent scale deposits. The alloy samples were 1 by 1-3/4-inches, and 1/16 inch thick or less. The materials were prepared in the same manner described for the 1974 test series. Scales and corrosion products were evaluated by X-ray diffraction, atomic absorption spectroscopy (AAS), and proton-induced X-ray emission. General-, pitting-, and crevice-corrosion and the susceptibility to stress-corrosion cracking were determined by weight-loss measurements and by microscopic examination.

TABLE 1. - Mean velocity and Reynolds number for brine and steam test packages

| Test package | Temperature, ° C | Pressure, psig | GTF flow rate, gpm | Package flow rate, pps | Velocity, fps | Reynolds No., X10$^6$ |
|---|---|---|---|---|---|---|
| P1: Input brine. | 232 | 315 | 75 | 10.38 | 4.2 | 5.36 |
| | | | 100 | 13.84 | 5.6 | 7.14 |
| P2: Brine..... | 205 | 230 | 75 | 9.35 | 3.71 | 4.25 |
| | | | 100 | 12.5 | 4.94 | 5.66 |
| P3: Steam..... | 205 | 230 | 75 | 1.05 | 41.1 | 4.11 |
| | | | 100 | 1.4 | 54.8 | 5.48 |
| P4: Brine..... | 165 | 120 | 75 | 8.4 | 3.15 | 2.72 |
| | | | 100 | 11.2 | 4.2 | 2.19 |
| P5: Steam..... | 165 | 120 | 75 | .94 | 85.6 | 2.73 |
| | | | 100 | 1.25 | 114. | 3.64 |
| P6: Steam..... | 100 | 15 | 75 | 1.05 | 593. | 5.06 |
| | | | 100 | 1.4 | 790. | 6.74 |
| P7: Steam..... | 100 | 15 | 75 | .94 | 533. | 4.5 |
| | | | 100 | 1.25 | 710. | 6.0 |

## RESULTS

### Salton Sea KGRA--1974

### Corrosion Measurements

Average corrosion rates, expressed as mils of surface thickness lost to corrosion per year of exposure (mpy), for the 1974 test samples are shown in table 2. (To convert mils per year to millimeters per year, multiply mpy by 0.0254). Typical conditions existing in the brine and steam packages are given in table 3 as compiled from San Diego Gas & Electric Co. (3) and Bureau of Mines field operations data. Conditions fluctuated considerably during the 500-hour corrosion test.

TABLE 2. - Corrosion rates for the samples exposed to Magmamax No. 1 well brine, 1974, mpy

| Alloy | Brine | Steam |
|---|---|---|
| 1020 carbon steel..... | 115 | 92 |
| 4130 steel..... | 31 | 109 |
| Hastelloy C-276..... | .8 | .0 |
| Inconel 625..... | .1 | .1 |

TABLE 3. - Typical conditions during 1974 field corrosion test, Magmamax No. 1 well

| | Corrosion test package | |
|---|---|---|
| | Brine | Steam |
| Temperature.....° C .. | 155 | 144 |
| Pressure.....psig.. | 50 | 48 |
| Total dissolved solids....mg/l.. | 297,800 | 120-1,500 |
| Chloride.....mg/l.. | 152,800 | 90-820 |

There were no differences in the measured corrosion rates between the samples exposed perpendicular to and those exposed tangential to the direction of flow. The 4130 steel and 1020 carbon steel samples corroded rapidly in the brine and steam phases. The 1020 carbon steel corroded at a higher rate in the brine than 4130 steel. Hastelloy C-276 and Inconel 625 showed little evidence of corrosion in either the brine or steam environment. Microscopic examination of the corroded surfaces revealed severe pitting of the 1020 carbon and 4130 steel samples. The deepest pit in 1020 carbon steel was 16 mils and the average value for the five deepest pits was 14 mils. The deepest pit in 4130 steel was 6.3 mils and the average value for the five deepest pits was 5.7 mils.

A statistical evaluation of the corrosion data from these initial field tests is not possible because only a few samples of each material were tested. Also, some of the sample mounting tees were opened at various times to visually inspect the samples. However, it was apparent that carbon and low alloy steels corrode rapidly in both the steam and the brine environments.

## Scale Characterization

All of the samples exposed to brine were covered with a hard black scale which was examined by X-ray diffraction, ESA, SEM, and PIXE. X-ray diffraction analyses showed that the scale contained two major crystalline phases, lead sulfide (galena) and sodium chloride (halite), and a substantial amount of amorphous material. There were no observable differences in the scales for the samples mounted perpendicular to or tangential to the brine flow. The low-alloy samples exposed to the steam were covered also with a thin, dark scale that was primarily magnetite.

Emmission spectrographic analysis of scales removed from corrosion samples exposed to the brine and the steam are shown in table 4. Wet chemical analyses of scales formed on samples exposed to the brine are shown in table 5. Scales removed from the different alloys had similar compositions except for their iron content. Hence, no distinction was made in the results for scales from the different alloys. Wet chemical and ESA analyses of scales formed in the brine are in reasonable agreement and show substantial amounts of silica, copper, lead, silver, manganese, and zinc.

TABLE 4. - ESA results for scales formed on corrosion samples, Magmamax No. 1 well, 1974

| Element | Concentration, wt-pct | |
|---|---|---|
| | Brine | Steam |
| Si..... | >10 | - |
| Fe, Cu, Pb..... | 1 -10 | - |
| Ag, Al, Mg, Mn, Zn..... | .1- 3 | - |
| Fe, Pb, Si<br>Zn, Mg, Mn } ..... | - | 0.01-1 |

TABLE 5. - Wet-chemical analysis of scales formed on corrosion test samples in brine, Magmamax No. 1 well, 1974,[1] wt-pct

| Element | Concentration range |
|---|---|
| Ag | 0.05- 0.53 |
| Al | .30- 1.20 |
| Cu | .57- 7.51 |
| Fe | 7.78-19.7 |
| Mn | .57- 6.51 |
| Pb | 4.42- 7.21 |
| Si | 15.1 -24.4 |
| Zn | .14- 1.88 |

[1]Analyses were not made for nonmetal (other than silicon) and minor metal components of the scale.

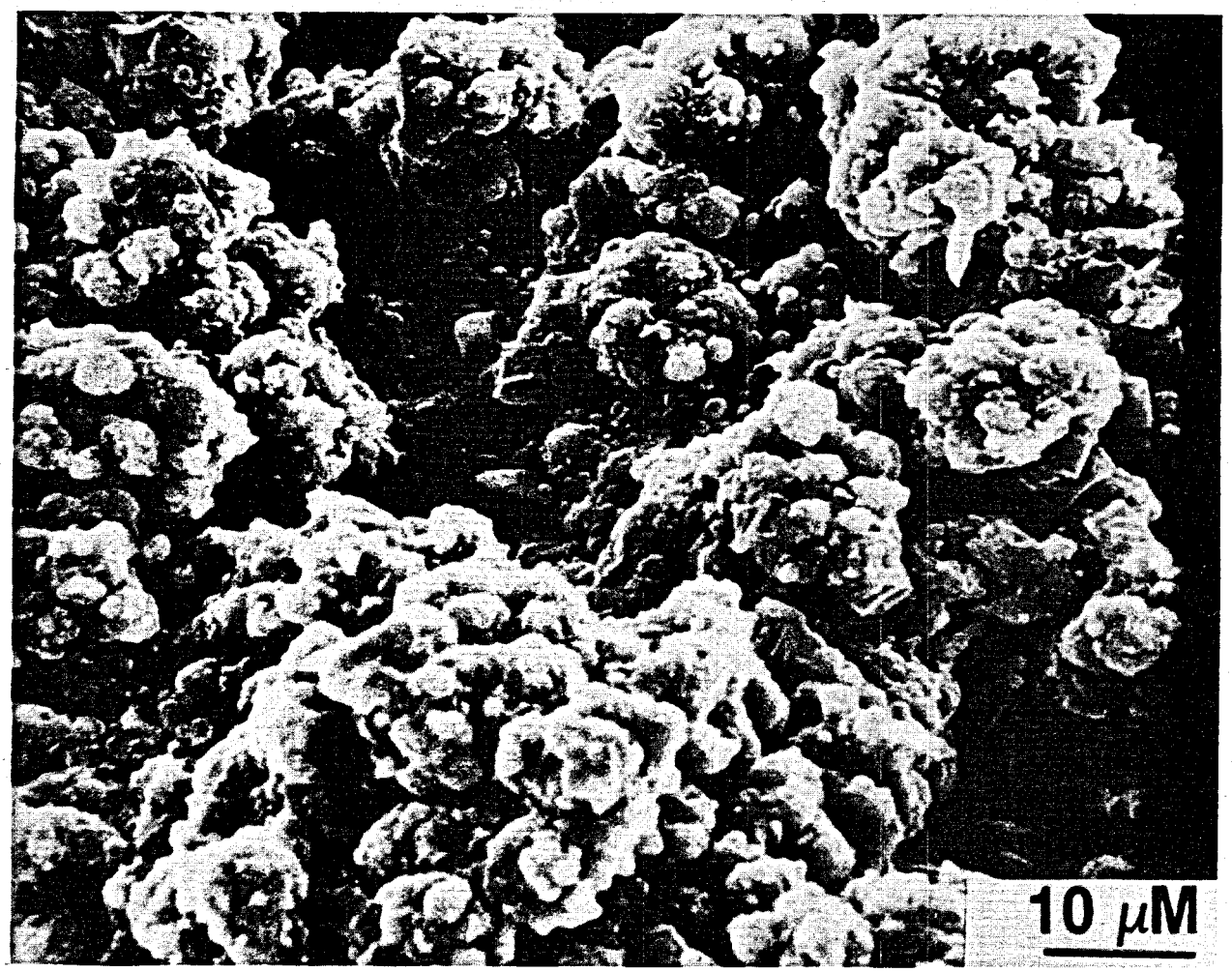

Scanning electron microscope examination of the scales formed in the brine showed that they were porous and were not an effective barrier to corrosion (fig. 12). Interconnecting pores penetrated to the sample surfaces, provided access of the brine to the metal, and favored nonuniform and localized corrosion such as pitting and crevice corrosion. Scale removed from samples that exhibited high corrosion rates, such as 1020 carbon steel, had a very rough texture at the scale-metal interface (fig. 13). Scales removed from samples exhibiting low corrosion rates, such as Hastelloy C-276, had a smooth texture at the scale-metal interface which tended to replicate the original texture of the sample surface (fig. 14). Because of the porous nature of the scale, it probably promoted localized corrosion in susceptible alloys.

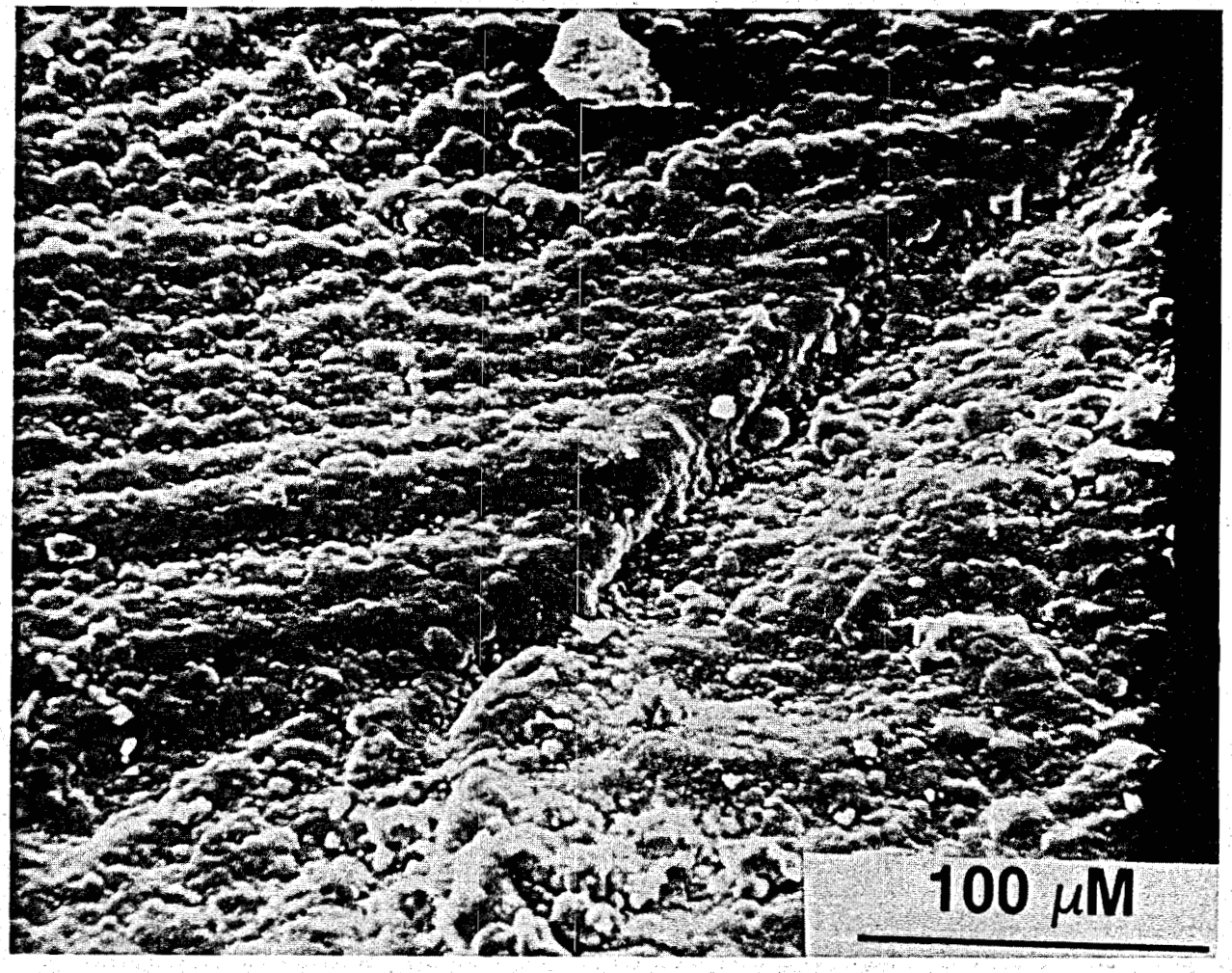


FIGURE 13. - SEM micrograph of scale-metal interface of scale removed from 1020 carbon steel sample, 1974.

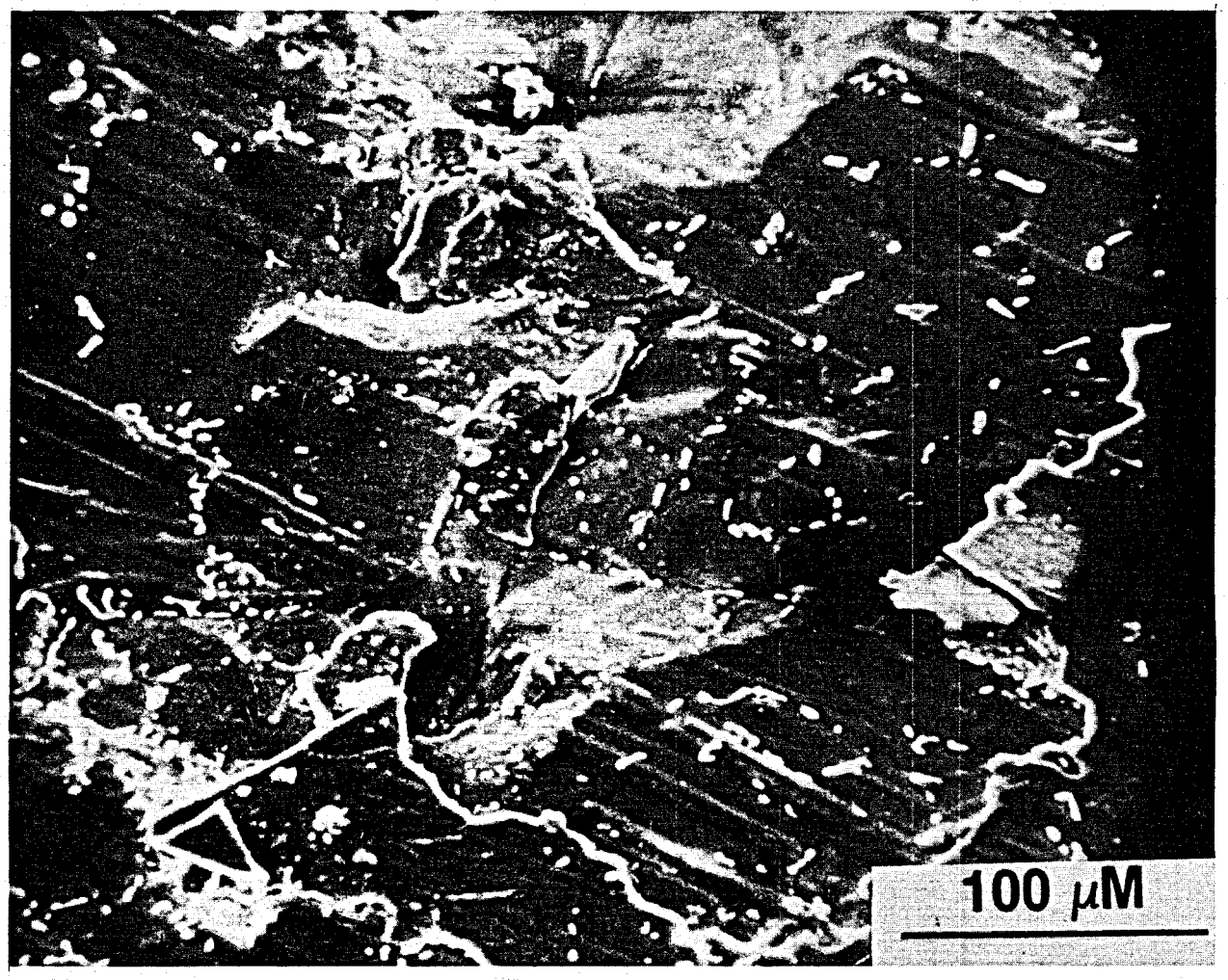


FIGURE 14. - SEM micrograph of scale-metal interface of scale removed from Hastelloy C-276 sample, 1974.

Proton-induced X-ray emission analyses of the outer 2,000 A of the scales formed in brine are shown in table 6. These results indicate that the composition of the outer layer of the scales is dependent on alloy composition. For example, the scales formed on 1020 carbon and 4130 steels had high iron concentrations in the outer layer, suggesting that the corrosion product readily diffused through the porous scale and distributed throughout it. However, none of the major alloying elements were detected in the outer 2,000 A of the scale formed on the more corrosion-resistant alloys Inconel 625 and Hastelloy C-276. These scales contained only those elements originally present in the brine.

TABLE 6. - Proton-induced X-ray emission analysis of outer 2,000 A of scales formed on corrosion samples in brine, Magmamax No. 1 well, 1974

| Alloy | Concentration in outer 2,000 A, at. pct | | | | | |
|---|---|---|---|---|---|---|
| | Ca | Cl | Fe | Na | Si | S |
| 1020 carbon steel..... | (1) | 12.6 | 84.0 | 0.8 | 2.1 | (1) |
| 4130 steel..... | (1) | 14.4 | 84.4 | 1.1 | (1) | (1) |
| Inconel 625..... | 5.6 | 47 | (1) | 24.0 | 16.7 | 5.6 |
| Hastelloy C-276..... | (1) | 15.6 | (1) | 12.5 | 20.3 | 12.4 |

[1]Not detected.

## Salton Sea KGRA--1976-77

General-, pitting, and crevice-corrosion and some stress-corrosion cracking results obtained by evaluation of the in situ weight-loss test samples are presented in this report; results from the U-bend, stress-corrosion samples are not. Mean operating conditions of the corrosion test packages, obtained by averaging the field operations data over the 30 days of the corrosion test series, are given in table 7 and are shown in figure 15 for the first five corrosion test packages. Conditions in packages P6 and P7 were controlled poorly and results are uncertain.

TABLE 7. - Mean conditions during 1976-77 field corrosion test

(Average flowrate into P1 from Magmamax No. 1 well = 45 gpm)

| Corrosion test package | Temperature, ° C | Pressure, psig | Chloride, ppm | pH[1] |
|---|---|---|---|---|
| Input brine, P1..... | 229 | 302 | 118,200 | 5.11 |
| Brine, P2..... | 207 | 224 | 123,000 | 5.68 |
| Steam, P3..... | 207 | 224 | 9,500 | 5.88 |
| Brine, P4..... | 178 | 140 | 128,000 | 5.73 |
| Steam, P5..... | 178 | 140 | 8,620 | 6.70 |
| Steam, after scrubbing tower, P6.... | 100 | 15 | [2]170 | (2) |
| Steam, after scrubbing tower, P7.... | 100 | 15 | [2]360 | (2) |

[1]pH measured at 25° C.
[2]Value is not known or is questionable.

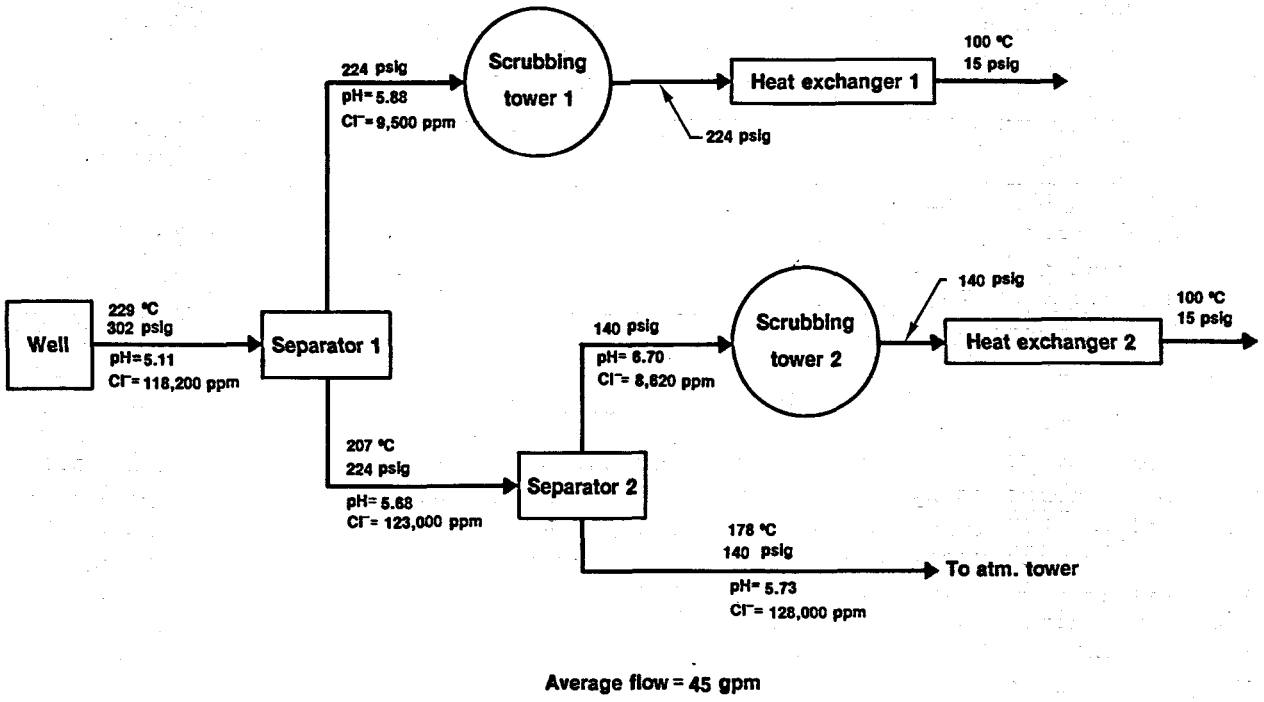


FIGURE 15. - Diagram showing the mean conditions during the field corrosion test series, Magmamax No. 1 well.

## Corrosion Measurements

### General Corrosion

General corrosion rates for two 15-day and one 30-day exposure periods of 1020 carbon steel, 4130 steel, E-Brite 26-1, 430 and 316 stainless steels, TiCode-12, and titanium-1.5 nickel are shown in table 8 for the three brine process streams of the GTF and the rates for the four steam process streams are given in table 9. Hastelloys G, S, and C-276, Inconel 625, and stainless steel alloys 29-4 and 6X corroded at 0.2 mpy or less in all of the process streams and therefore were not included in these tables. Except in the few cases noted where the results for the two 15-day tests were widely different, the 15-day results are the average of the results from both tests. Individual corrosion rates generally varied less than 10 pct from these reported averages. Because air may have intruded into steam packages P6 and P7 for significant periods of time during the 15- and 30-day tests, there is uncertainty about the actual conditions of the test for these two packages. Results from P7 for the 30-day exposure have been reported as the range of measured corrosion rates.

Type 430 stainless steel had excellent corrosion resistance in the concentrated brine from the first-stage separator (P2) and, except for one of the 15-day tests, in the input brine (P1). The corrosion rate of 430 stainless steel in the other packages appeared to increase with time. In steam package P7, the corrosion rate of 430 stainless steel varied considerably from sample to sample for the 30-day period.

TABLE 8. - General corrosion rates (mpy) in the brine test packages, 15- and 30-day tests, Magmamax No. 1 well, 1976-77[1]

| Alloy | P1[2] | | P2[2] | | P4[2] | |
|---|---|---|---|---|---|---|
| | 15 days | 30 days | 15 days | 30 days | 15 days | 30 days |
| 1020 carbon steel | 67 | 43 | [3]27 -62 | 42 | 48 | 39 |
| 4130 steel | [3]13 -33 | [3]4-37 | [3]3.6- 6.8 | [3]6.6-57 | [3]2.2-10.3 | 3.1 |
| 430 stainless steel | [3].6- 2.2 | .5 | .2 | .3 | .6 | 1.1 |
| 316 L stainless steel | .7 | .3 | .1 | .4 | .3 | .2 |
| E-Brite 26-1 | .2 | .2 | .2 | .3 | .0 | .1 |
| TiCode-12 | .0 | .7 | .0 | 1.9 | .3 | 1.1 |
| Titanium-1.5 nickel | .0 | ([4]) | ([4]) | ([4]) | ([4]) | ([4]) |

[1]15-day rates are the averages for 4 to 5 samples in each of two 15-day sequences; 30-day rates are the averages for 8 samples.

[2]P1--input brine; P2--brine from first-stage steam separator; P4--brine from second-stage steam separator.

[3]Results for 2 tests are reported separately because of wide differences in the observed corrosion rates.

[4]Not tested.

TABLE 9. - General corrosion rates (mpy) in the steam test packages, 15- and 30-day tests, Magmamax No. 1 well, 1976-77[1]

| Alloy | P3[2] | | P5[2] | | P6[2] | | P7[2] | |
|---|---|---|---|---|---|---|---|---|
| | 15 days | 30 days | 15 days | 30 days | 15 days | 30 days | 15 days | 30 days |
| 1020 carbon steel | 26 | 28 | 25 | 28 | [3]21-40 | 25 | [3]18-27 | 30-79 |
| 4130 steel | 7.7 | 13 | 8.2 | 12 | 18 | 18 | 25 | 27-52 |
| 430 stainless steel | .8 | 2.0 | .5 | 1.2 | .4 | 1.0 | 1.4 | 3.9- 7.8 |
| 316 L stainless steel | .4 | .2 | .3 | .5 | .2 | .2 | .2 | .3- 1.0 |
| E-Brite 26-1 | .3 | .3 | .3 | .4 | .2 | .3 | .1 | .4 |
| TiCode-12 | 0 | 1.9 | .7 | 1.8 | ([4]) | .5 | ([4]) | ([4]) |
| Titanium-1.5 nickel | ([4]) | ([4]) | ([4]) | ([4]) | 0 | .6 | ([4]) | ([4]) |

[1]15-day rates are the averages for 4 to 5 samples in each of two 15-day sequences; 30-day rates are the averages for 8 samples.

[2]P3--steam from the first-stage steam separator; P5--steam from second-stage steam separator; P6-P7--steam from the first- and second-stage steam scrubbers, respectively.

[3]Results for 2 tests are reported separately because of wide differences in the observed corrosion rates.

[4]Not tested.

The 1020 carbon and 4130 alloy steels exhibited fairly high corrosion rates in all of the test environments. Corrosion rates were generally higher in the brines than in the steam phase. However, corrosion rates of 1020 carbon and 4130 alloy steels decreased with exposure time in the brine, whereas corrosion rates increased in the steam phase.

E-Brite 26-1 exhibited good resistance to general corrosion in all of the environments. Type 316 L stainless steel also had good resistance to general corrosion but the results from steam package P7 were somewhat erratic. Microscopic examination, however, showed that 316 L stainless steel was susceptible to intergranular corrosion in all of the process environments (fig. 16). General corrosion rates for the titanium alloys were low but increased signicantly with time of exposure in both the brine and steam environments.

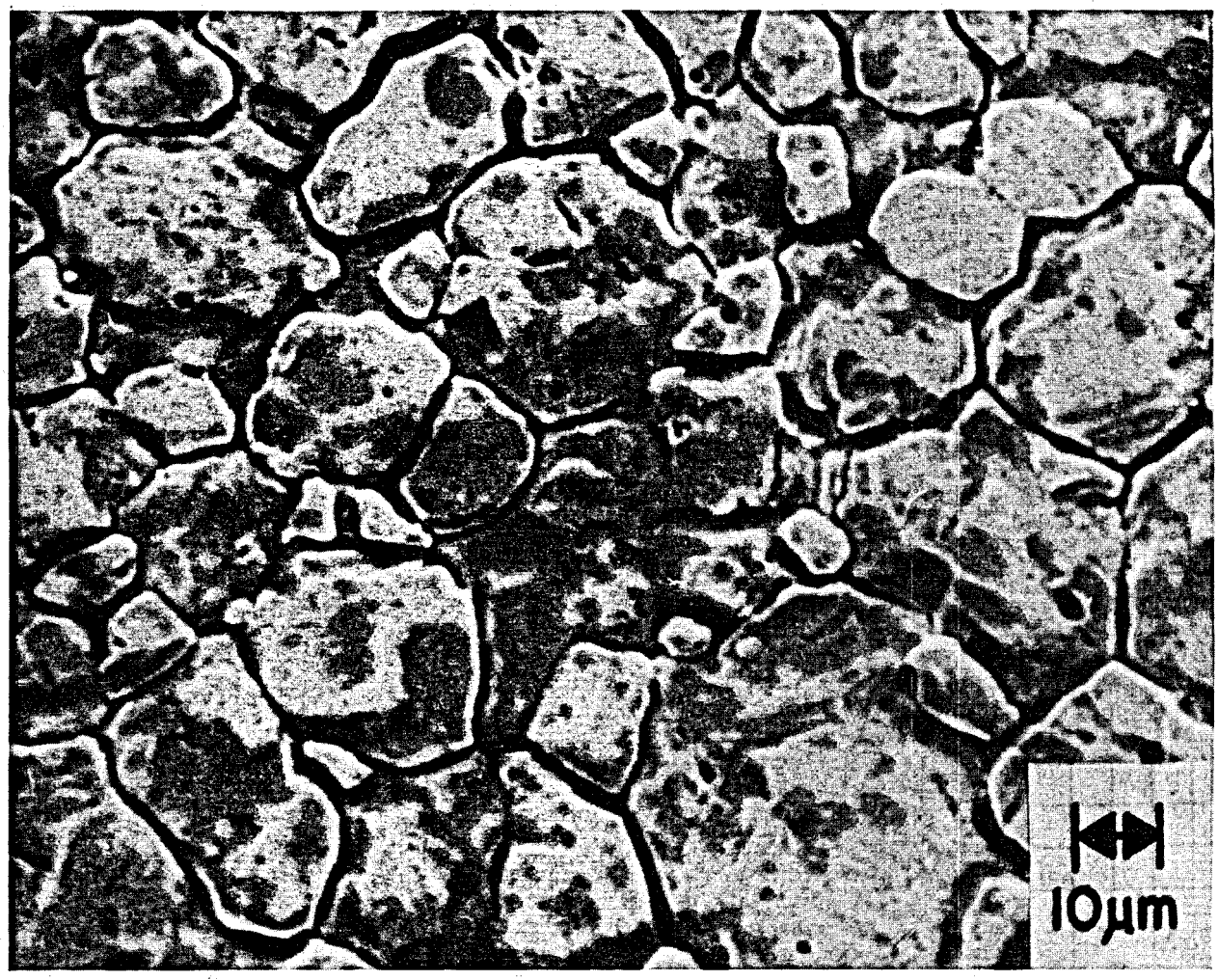


FIGURE 16. - SEM micrograph showing intergranular corrosion of 316 L stainless steel exposed to brine from steam separator 1 (30-day exposure), 1976-77.

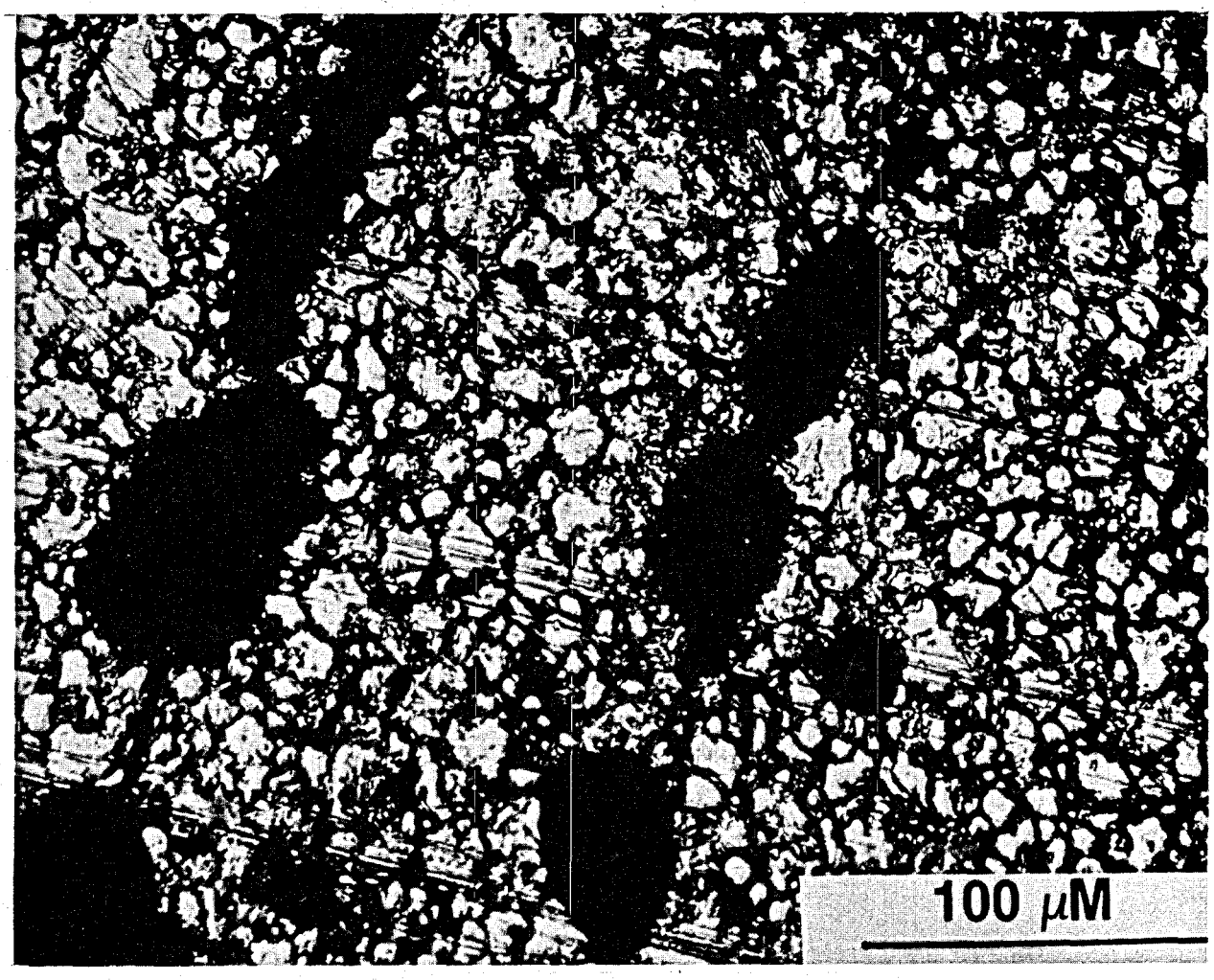


FIGURE 17. - Photomicrograph showing pitting in surface of 316 L stainless steel sample exposed 30 days to input brine, 1976-77.

Pitting Corrosion

Nickel- and titanium-based alloys did not pit in the brine or steam environments during the 15- or 30-day tests. However, except for alloy 29-4, all of the iron-based alloys pitted in the seven process environments of the GTF. The maximum and average pit depths (measured with an optical micrometer) for the iron-based alloys are shown in tables 10-11. In the 15-day tests, 1020 carbon and 4130 alloy steels exhibited greater pit depths in the brines than in the steam phases, while the opposite was true for the high-alloy steels. The 30-day-test results showed the 1020 carbon and 4130 alloy steels continued to pit more readily in the brines than in the steams while the pit depths for the high-alloy steels in the brine and steam environments were similar. In general, pit depths increased with exposure time and, in some cases, notably 316 L stainless steel (fig. 17), pit depths increased by a factor of 5 while exposure time only doubled. In the case of 316 L stainless steel from steam package P3, the pitting rate computed from the average pit depth for a 30-day exposure was 45 mpy, more than 200 times the general corrosion rate reported for this alloy in table 9.

TABLE 10. - Maximum and average pit depths (mils) for samples exposed to brine, 15- and 30-day tests, Magmamax No. 1 well, 1976-77[1]

| Alloy | P1[2] | | | | P2[2] | | | | P4[2] | | | |
|---|---|---|---|---|---|---|---|---|---|---|---|---|
| | 15 days | | 30 days | | 15 days | | 30 days | | 15 days | | 30 days | |
| | Maximum | Average | Maximum | Average | Maximum | Average | Maximum | Average | Maximum | Average | Maximum | Average |
| 1020 carbon steel..... | 7.3 | 6.8 | [3]22.4 | 14.8 | 11.8 | 8.5 | [3]14.3 | 12.3 | 9.7 | 7.7 | [3]13.6 | 12.5 |
| 4130 steel..... | [3]6.1 | 3.0 | [3]7.1 | 4.9 | 4.2 | 2.7 | 8.1 | 6.1 | 3.6 | 3.1 | 8.7 | 7.2 |
| 430 stainless steel..... | 4.2 | 2.8 | 3.8 | 3.0 | 3.3 | 1.6 | 3.1 | 2.3 | 1.7 | .9 | 4.6 | 3.6 |
| Alloy 6X..... | 0 | 0 | 1.5 | .8 | 0 | 0 | 1.0 | 0.5 | 1.2 | .7 | 3.0 | 2.0 |
| E-Brite 26-1..... | 3.5 | 1.0 | 3.5 | 2.8 | 4.7 | 2.1 | 5.0 | 3.5 | 1.6 | .9 | 3.7 | 3.1 |
| 316 L stainless steel[4]... | 2.8 | 1.9 | [5]3.0 | 2.2 | [6]1.1 | .8 | [5]3.0 | 1.8 | 1.8 | .9 | [5]4.5 | 3.6 |

[1]Average for 4 to 5 samples using 5 deepest pits on each sample.
[2]P1--input brine; P2--brine from first-stage separator; P4--brine from second-stage separator.
[3]Pitting on edges.
[4]Intergranular corrosion observed.
[5]Cracks penetrate completely through sample thickness.
[6]Microcracks on surface observed.

TABLE 11. - Maximum and average pit depths (mils) for samples exposed to steam, 15- and 30-day tests, Magmamax No. 1 well, 1976-77[1]

| Alloy | P3[2] | | | | P5[2] | | | |
|---|---|---|---|---|---|---|---|---|
| | 15 days | | 30 days | | 15 days | | 30 days | |
| | Maximum | Average | Maximum | Average | Maximum | Average | Maximum | Average |
| 1020 carbon steel..... | [3]6.2 | 5.5 | [3]12.0 | 9.0 | 8.3 | 6.0 | 13.9 | 11.8 |
| 4130 steel..... | 3.2 | 2.6 | [3]6.0 | 4.6 | 4.5 | 4.2 | 9.3 | 7.3 |
| 430 stainless steel..... | 3.6 | 2.7 | 4.2 | 3.1 | 4.1 | 3.7 | 9.1 | 5.3 |
| Alloy 6X..... | 1.6 | .9 | 2.0 | 1.5 | 1.5 | 1.0 | 2.9 | 2.2 |
| E-Brite 26-1..... | 3.7 | 1.9 | 4.2 | 3.1 | 4.2 | 2.5 | 7.4 | 4.5 |
| 316 L stainless steel[4]..... | [5]1.3 | .8 | [6]5.8 | 5.8 | [5]3.4 | 2.2 | [6]5.9 | 4.3 |
| | P6[2] | | | | P7[2] | | | |
| 1020 carbon steel..... | 3.4 | 2.4 | 11.6 | 9.5 | 5.7 | 3.5 | [3]7.0 | 4.3 |
| 4130 steel..... | 4.0 | 3.0 | 10.3 | 6.3 | 6.3 | 3.9 | [3]6.4 | 5.5 |
| 430 stainless steel..... | 5.0 | 3.7 | 10.4 | 7.6 | 12.5 | 5.0 | [3]12.7 | 9.2 |
| Alloy 6X..... | 1.5 | 1.2 | 3.9 | 2.9 | 1.2 | .9 | 1.6 | .8 |
| E-Brite 26-1..... | 2.3 | 1.8 | 7.5 | 5.0 | 9.8 | 2.4 | [3]14.4 | 10.2 |
| 316 L stainless steel[4]..... | 5.2 | 2.9 | 6.4 | 5.4 | 10.9 | 9.0 | [3]22 | 13.2 |

[1]Average for 4 to 5 samples using 5 deepest pits on each sample.
[2]P3--steam from first-stage separator; P5--steam from second-stage separator; P6-P7--steam from first- and second-stage scrubbers, respectively.
[3]Pitting edges.
[4]Intergranular corrosion observed.
[5]Microcracks on surface observed.
[6]Cracks penetrate completely through the sample thickness.

## Crevice Corrosion

Although precautions were taken in mounting the samples for testing to avoid crevices, crevice corrosion occurred beneath the ceramic insulators on a number of alloys (table 12). Crevice corrosion took the form of accelerated general or pitting corrosion beneath the ceramic insulators. Table 12 shows that crevice attack was least likely to occur in the input brine package (P1) and most likely to occur in the steam package (P7).

TABLE 12. - Crevice corrosion, 15- and 30-day tests, Magmamax No. 1 well, 1976-77

| Alloy | P1 | | P2 | | P3 | | P4 | | P5 | | P6 | | P7 | |
|---|---|---|---|---|---|---|---|---|---|---|---|---|---|---|
| | 15 days | 30 days | 15 days | 30 days | 15 days | 30 days | 15 days | 30 days | 15 days | 30 days | 15 days | 30 days | 15 days | 30 days |
| 1020 carbon steel..... | N | N | N | N | N | N | N | N | N | N | D | N | D | N |
| 4130 steel..... | N | N | N | N | N | N | N | N | N | N | N | N | D | N |
| 430 stainless steel..... | N | N | D | D | D | D | D | D | D | D | N | N | D | N |
| Alloy 6X..... | N | N | D | N | N | N | N | N | D | D | N | N | D | N |
| E-Brite 26-1..... | N | N | D | D | D | D | D | D | D | D | N | N | D | N |
| 316 L stainless steel..... | D | D | D | D | N | N | D | N | D | N | D | D | D | N |
| Alloy 29-4..... | N | N | N | N | N | N | N | N | N | D | N | N | N | N |
| Hastelloy G..... | N | N | N | D | N | D | N | N | N | N | D | N | N | D |
| Hastelloy S..... | N | N | N | N | N | N | N | N | N | N | N | N | D | D |

N = Not detected.
D = Detected.

## Stress Corrosion Cracking

During the 15-day tests, 316 L stainless steel weight-loss coupons developed microcracks on exposure in some test packages (tables 10-11). Examination of the 30-day samples showed that the microcracks had grown and in some cases penetrated completely through the sample thickness (fig. 18). It can be seen from figure 18 that the cracks have the branch structure typical of stress-corrosion cracking. Examination of the cracks at higher magnification (fig. 19) showed that the cracks were transgranular. The cause for transgranular stress corrosion cracking in these samples was probably an increase in the residual stresses in the metal due to cold working during sample preparation. Stress corrosion cracking of type 316 L stainless steel in these environments has been reported previously (4-5).

## Equipment Corrosion Failures

During the period from June 1976 until October 1976, the GTF was operated continuously as various system components were tested, modified, and brought online. Except for a 4-day period in October 1976, when Woolsey No. 1 well was used as the source of brine, the brines from Magmamax No. 1 well were used at many pressures, temperatures, and flow rates. Although there were no scheduled corrosion tests in the MTF during this period, corrosion-related failures of various process equipment components occurred.

A typical example was the failure of a 3-inch-diameter schedule-40 mild steel pipe elbow located on the MTF bypass line. This bypass line was used to maintain the total flow rate from Magmamax No. 1 well at a constant value while the flow rate through the materials test facility was varied. After 30 hours use, during which time considerable flashing of the brine occurred

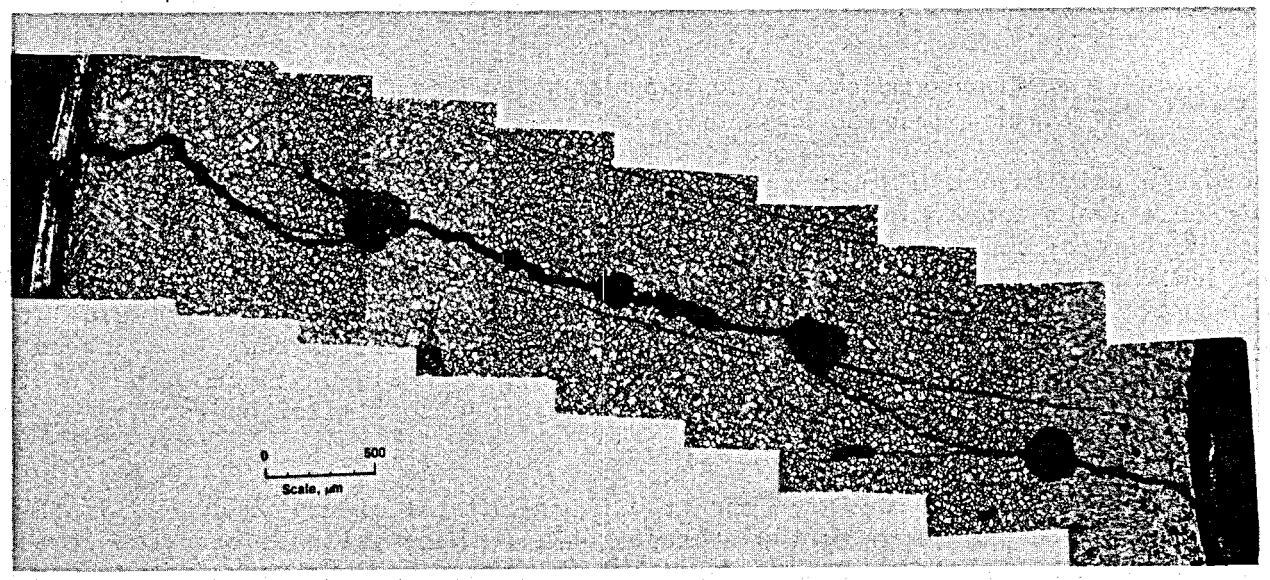


FIGURE 18. - Composite photomicrograph showing crack in surface of 316 L stainless steel sample exposed 30 days to brine from steam separator 2, 1976-77.

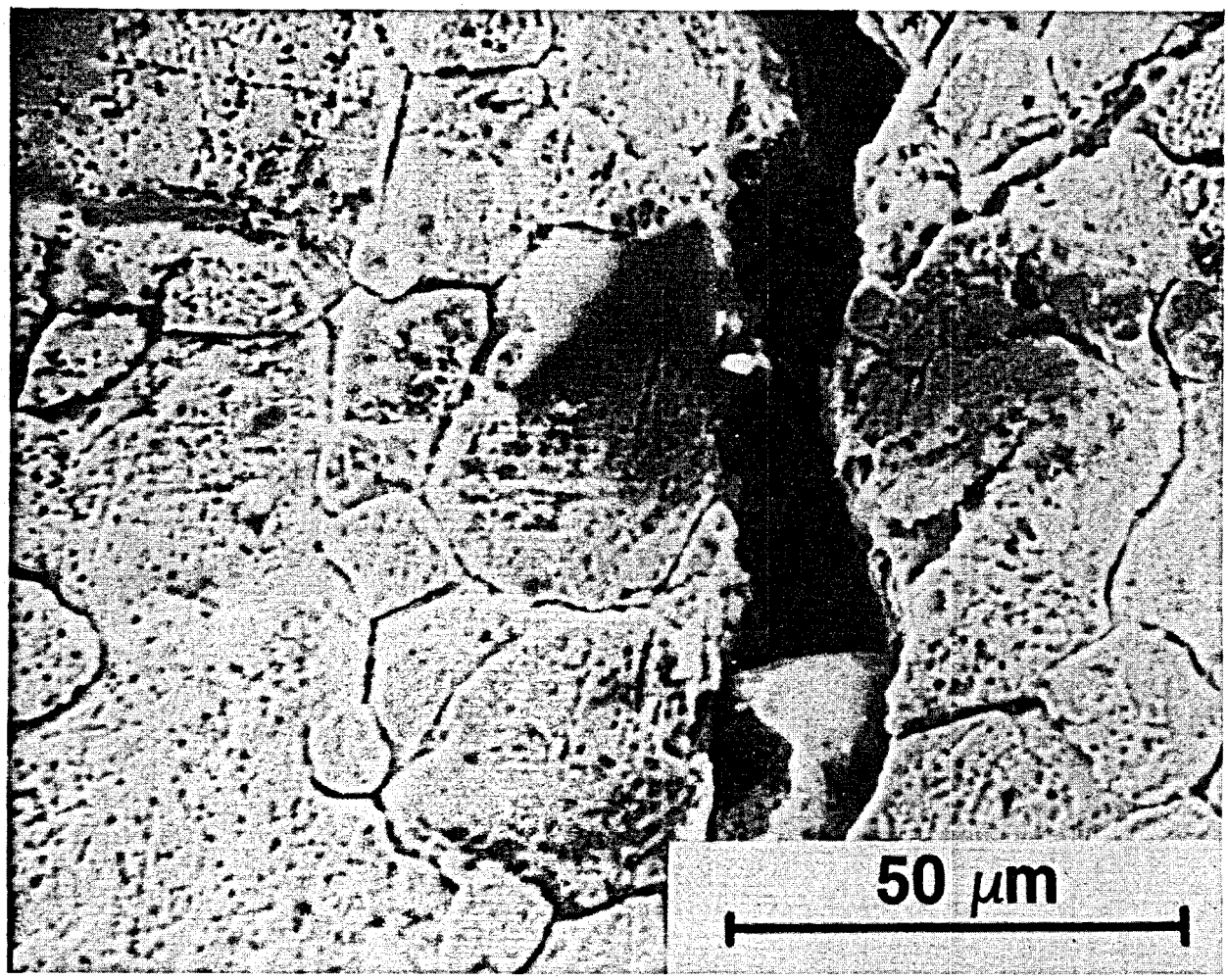


FIGURE 19. - SEM micrograph showing transgranular cracking in surface of 316 L stainless steel sample exposed 30 days to brine from steam separator 2, 1976-77.

across a valve about 10 inches upstream from the elbow, the elbow failed when pin-hole leaks appeared at the vertex of the right angle bend (figs. 20-21). At the time of failure, approximately 80,000 gallons of brine at 220° C had passed through the elbow. Cross sections of the elbow showed that the failed area was severely pitted and eroded. The failed area coincided with the point of impact of the flowing brine and steam on the pipe wall as the fluid passed through the 90° bend. Identical failures occurred at elbows in other parts of the GTF and the SDG&E facility which were subjected to similar operating conditions.

Corrosion fatigue failures occurred along several of the welded mild steel joints on one of the brine storage tanks. These failures occurred at a time when brine from the second-stage separator and from the bypass line were being flashed directly to atmospheric pressure in the storage tank, which was equipped with a series of baffle plates. The fatigue cracks were 1 to 6 inches long and developed at several locations over a distance of 20 feet

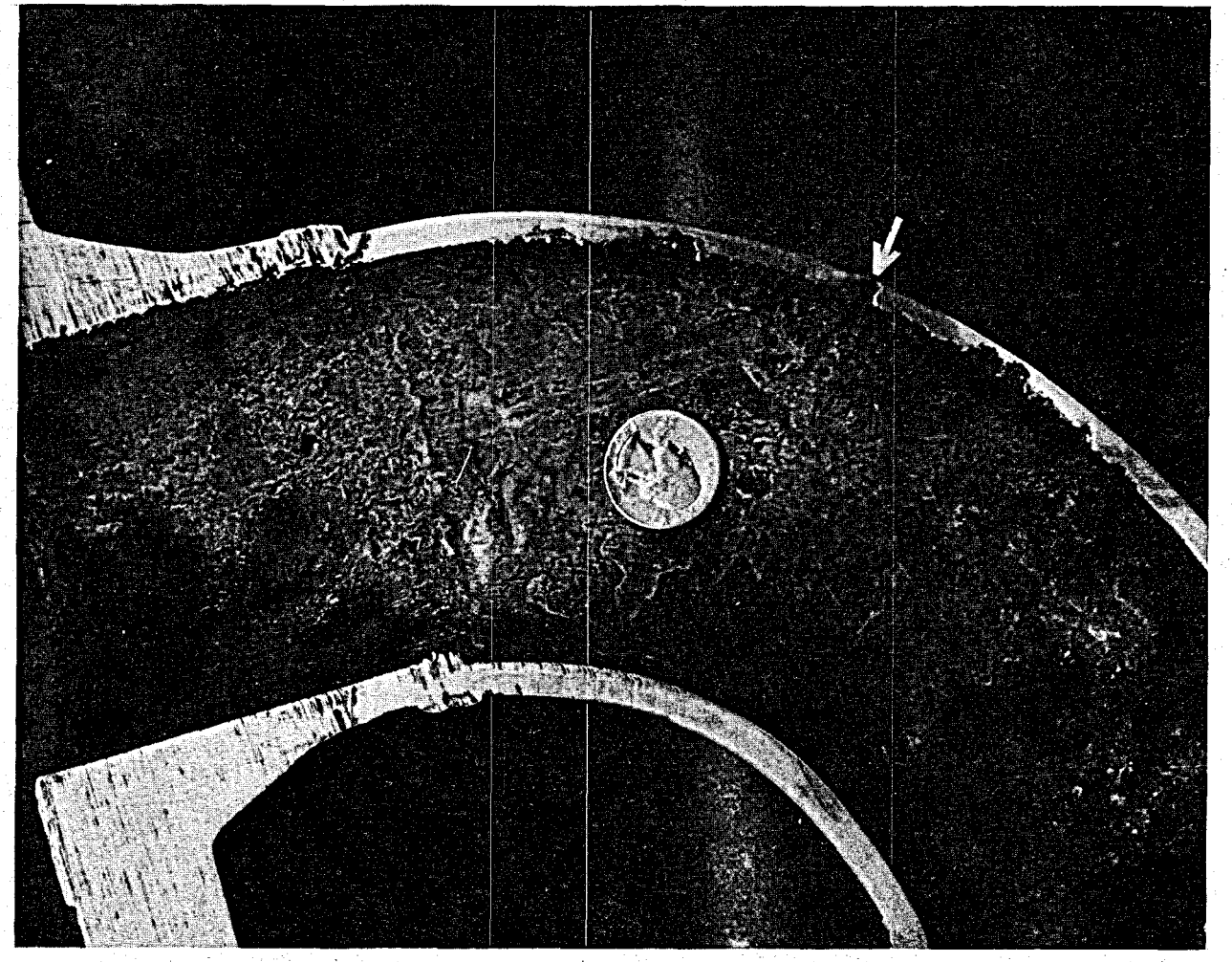

FIGURE 20. - Cross section of 3-inch elbow removed from input brine line showing erosion and pitting corrosion, 1976-77.

along one side of the tank. They were caused by intense vibrations occurring in the storage tank as the brines, typically 190° to 230° C and 100 to 250 psig, flashed to atmospheric pressure. Subsequent installation of the 30-ft-high atmospheric pressure flashing tower upstream from the brine storage tank eliminated the vibrations and recurrence of the fatigue cracks.

Another example is the failure of 1/8-inch-diameter E-Brite 26-1 tubing used by Magma Power Co. to suspend a pressure-temperature probe downhole in Magmamax No. 1 well during well-logging. The tubing failed after only a short period of use. Figure 22 shows a composite longitudinal cross section of the failed tubing. From left to right, figures 22A and 22B depict a metallurgical defect between the inner and outer walls of the tubing. The inside of the tube is the upper portion and the dark line through the tubing is the metallurgical defect. Based on the elongated structure of the defect, it was formed probably during extrusion or existed in the original metal billet and extended through the tube during forming operation. It can be seen from figure 22 that extensive pitting occurred along the defect as well as inside the tube.


FIGURE 21. - Detail of pitting failure in 3-inch elbow, 1976-77.

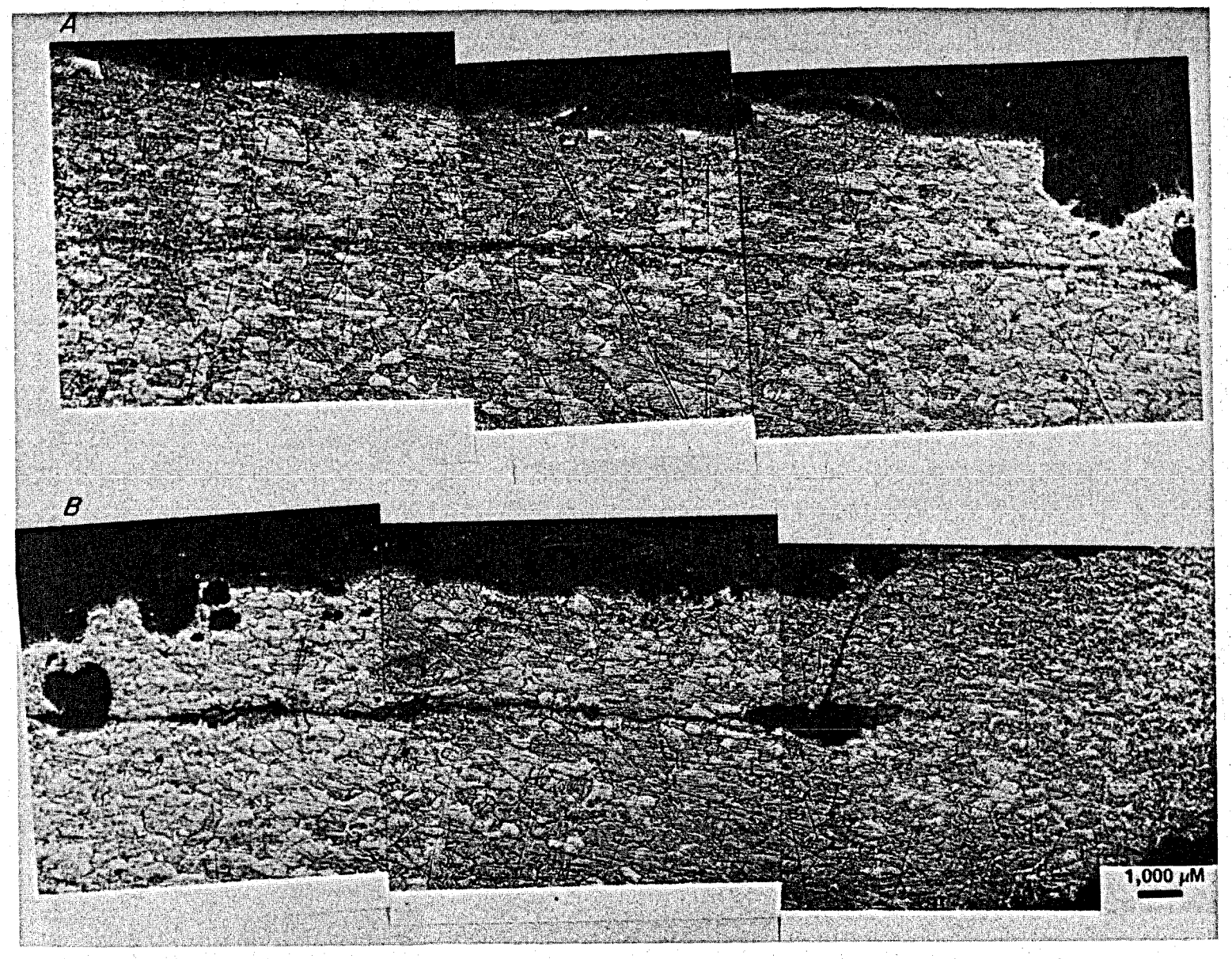


FIGURE 22. - Longitudinal cross section of E-Brite 26-1 tubing used in well-logging. Photographs *A* and *B*, left to right, depict massive pits along a continuous defect between the inner wall, top of the photographs, and the outer wall.

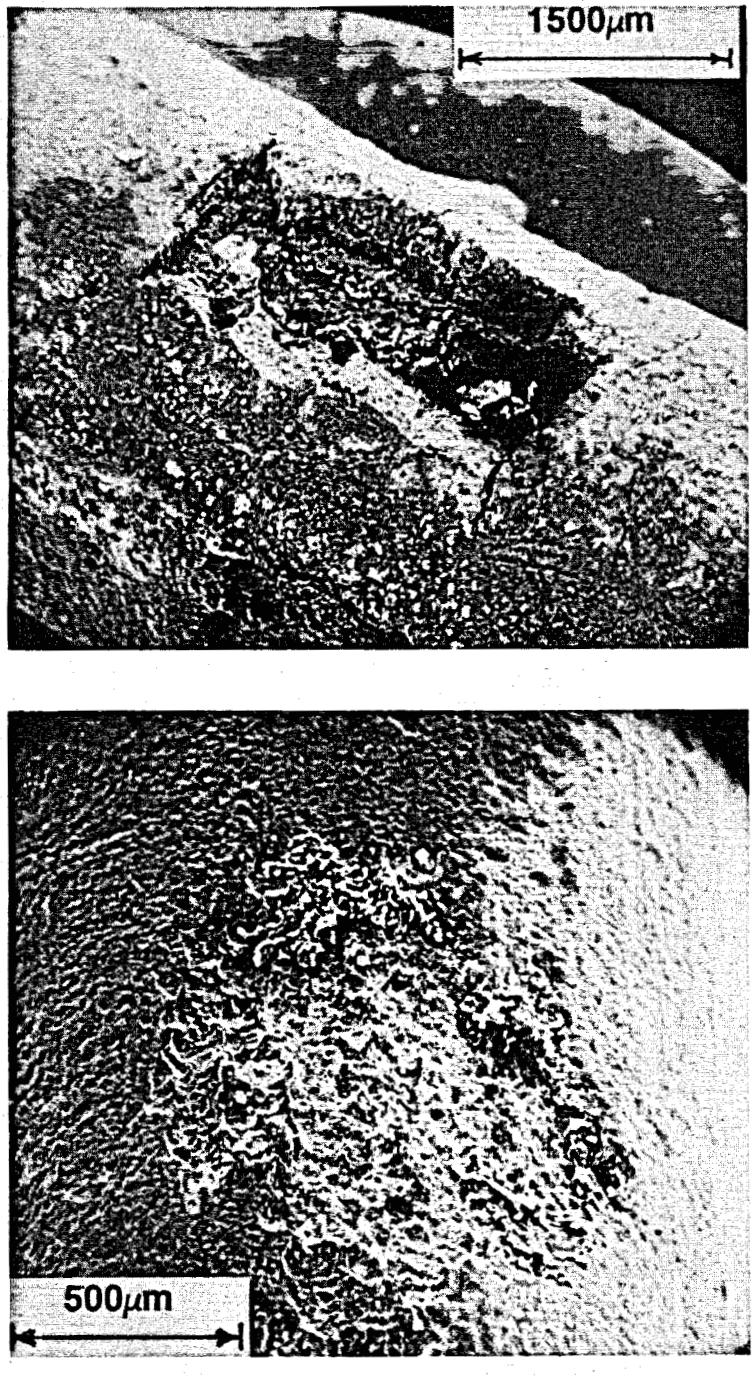


FIGURE 23. - SEM micrographs showing cracked and broken scale deposit on the outer surface of E-Brite 26-1 tubing used in well-logging *(A)*. Removal of scale from tubing showed local corrosion had begun in the area of the cracked and broken scale *(B)*, 1976-77.

A relatively thick scale had formed also around the outside wall of the E-Brite 26-1 tubing during the well-logging operation. This scale tended to break away during the insertion and removal of several thousand feet of the tubing in Magmamax No. 1 well. Figure 23 shows a SEM micrograph of a section of tubing where the scale had broken away, thereby exposing the tubing wall (fig. 23A) to the brine. The exposed metal underwent dissolution at this point with local corrosion being initiated (fig. 23B).

Pitting essentially occurred on four surfaces of the tube. This, coupled with the data for E-Brite 26-1 shown in table 10, indicates that half or more of the wall thickness could be penetrated in 15 days or less. A reduction of wall thickness of this magnitude and the accompaning loss of strength would result in total failure of the metal.

## Brine Chemistry

Samples of brine from Magmamax No. 1 well were obtained at regular intervals and analyzed using atomic absorption spectroscopy (AAS) and wet chemical techniques. The average composition of the input brine, over the period June 1976 through January 1977, is given in table 13 along with pH (measured at 25° C) and geothermal well flow-rate. Brine flow rates through the GTF averaged 50 gpm or less

during this period with the balance of the flow from the well being consumed by other users, primarily SDG&E. The mean chloride concentration and pH of the brine and condensed steam phases representing the seven process streams are given in table 7 and are shown in figure 15.

TABLE 13. - Average composition of brine from Magmamax No. 1 well during a 7-month period,[1] ppm

| Element | 1976 | | | | 1977 |
|---|---|---|---|---|---|
| | June 500 gpm[2] | August 150 gpm[2] | September-October 400 gpm[2] | October-November 500 gpm[2] | January 400 gpm[2] |
| Na | 46,200 | 46,900 | 47,000 | 47,900 | 51,300 |
| Ca | 61,500 | 17,400 | 21,200 | 22,116 | 21,100 |
| K | 7,360 | 9,310 | 10,400 | 8,770 | 10,400 |
| Sr | 415 | 783 | ([3]) | 725 | ([3]) |
| Li | 192 | 149 | ([3]) | 170 | ([3]) |
| Fe | 273 | 451 | 330 | 265 | 280 |
| Cu | ([3]) | ([3]) | .5 | .5 | .5 |
| Pb | 77 | ([3]) | 51 | 51 | 44 |
| Ag | ([3]) | ([3]) | ([3]) | .6 | .8 |
| Mg | ([3]) | ([3]) | ([3]) | 95 | 100 |
| Mn | ([3]) | ([3]) | 720 | 617 | 635 |
| Zn | ([3]) | ([3]) | 290 | ([3]) | 220 |
| Si | ([3]) | ([3]) | 239 | ([3]) | ([3]) |
| Ba | ([3]) | ([3]) | 140 | ([3]) | ([3]) |
| pH[4] | 5.3 | 5.2 | 5.2 | 5.1 | 5.5 |
| $Cl^-$ | 130,000 | 114,000 | 129,000 | 95,780 | 128,700 |

[1]For some of the elements, the analytical results obtained during the same period by San Diego Gas and Electric Co. have been included in the data.
[2]Flow rates are the total flow rate to all users of the well.
[3]Not determined
[4]pH measured at 25° C.

## Scale Characterization

Results of X-ray diffraction analyses of the scales formed on the corrosion samples in the seven process streams are shown in table 14 and elemental analyses obtained by AAS are shown in table 15. There was a difference in the composition of the scales formed in the scrubbed steam packages, P6 and P7, during the 15- and 30-day tests. Galena (PbS) was the major phase present on the samples after 15 days and magnetite was the major phase after 30 days. There were differences in the composition of the scales formed in each of the different environments. Galena was the principal crystalline phase present in the scales of samples removed from corrosion test packages P1 through P5. There was also an amorphous phase identified by Barnes, et al. (1) as an aluminosilicate material. There were, however, no significant differences in the composition of the scale formed on different alloy samples in the same environment. Referring to the mineral content of the scales, Barnes described the scales as very rich ores (1).

TABLE 14. - X-ray diffraction analysis of scales formed on 30-day corrosion test samples

| Corrosion test package | Mineral phases |
|---|---|
| P1 | Galena (major). Halite. |
| P2 | Galena (major). Halite. |
| P3 | Galena (major). Sphalerite. Magnetite. |
| P4 | Galena (major). Halite. |
| P5 | Mostly amorphous. Galena. |
| P6 | Magnetite (major). Calcite. |
| P7 | Magnetite-franklinite (major). Calcite. |

TABLE 15. - Atomic absorption spectroscopy analyses of scales formed on corrosion samples in five of the process streams,[1] wt-pct

| Element | Test package[2] | | | | |
|---|---|---|---|---|---|
| | P1 | P2 | P3 | P4 | P5 |
| Ag | 0.129 | 0.029 | 0.016 | 0.075 | 0.022 |
| Al | .014 | .36 | .25 | 1.03 | .18 |
| As | .04 | .06 | .03 | .10 | .08 |
| Ca | .26 | .55 | .53 | .87 | 1.12 |
| Cu | .024 | .32 | .63 | .87 | 1.12 |
| Fe | 1.95 | 5.97 | 8.37 | 6.49 | 27.7 |
| K | .17 | .34 | .28 | .76 | .56 |
| Mn | .10 | .63 | .39 | .89 | .27 |
| Na | .35 | .97 | .98 | 2.48 | 2.02 |
| Pb | 76.0 | 58.1 | 23.5 | 31.8 | 22.8 |
| Sb | .06 | .07 | .03 | .19 | .05 |
| Si | .90 | 2.63 | 2.50 | 7.02 | 6.64 |
| Zn | .12 | .56 | 11.7 | .45 | 1.42 |

[1]Analyses were not made for nonmetal (other than silicon) and minor metal components of the scale.

[2]P1--wellhead brine; P2 and P3--brine and steam from first separator, respectively; P4 and P5--brine and steam from second separator respectively.

The outer surface (first 2,000 A) of the scales formed on seven alloys--1020 carbon steel, 4130 steel, 430 stainless steel, stainless alloys 29-4 and 6X, and Hastelloys G and C-276--in the seven process environments were examined by PIXE analysis. These results were similar to those obtained by AAS (table 15) in that lead was found to be the most abundant element present. However, iron was detected in the outer layer of the scale formed on 1020 carbon steel, 4130 steel, and 430 stainless steel in the three brine packages (P1, P2, and P4). The scale formed on the other four alloys showed no concentration of iron or other alloy constituents in the outer surface region. These PIXE results are similar to those described for the samples of 1020 carbon and 4130 steels exposed to the concentrated brine from SDG&E second-stage separator during the 1974 tests (table 6). SEM examination of the galena-based scales indicated that they were quite porous. A cross-section (fig. 24) of scale formed in the input brine package, P1, showed that the scale contained extensive and interconnecting voids allowing the brine to penetrate to the metal surface. This was also a feature of scales deposited from the brine in the 1974 tests (fig. 12).

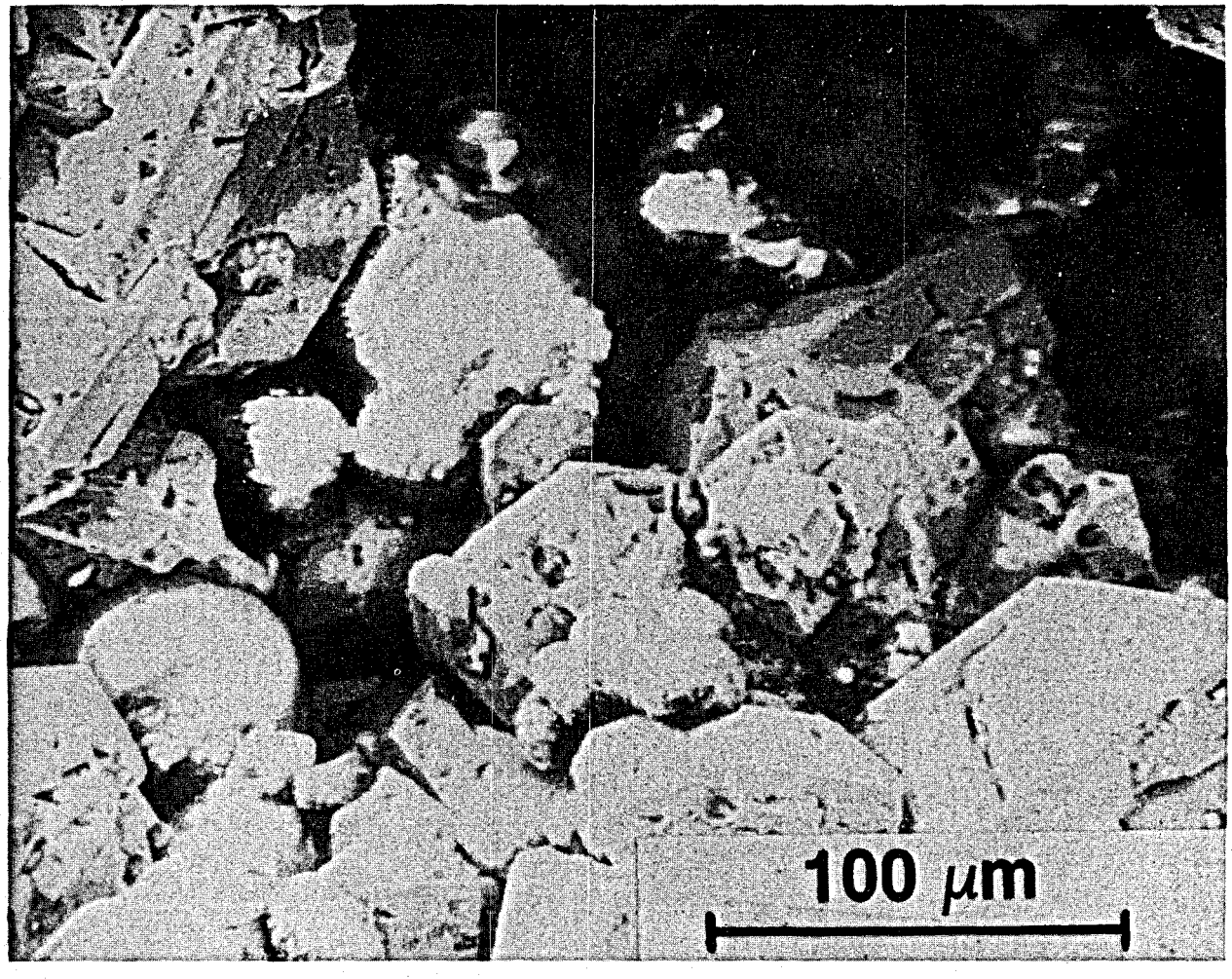


FIGURE 24. - SEM micrograph showing cross section of galena scale formed on corrosion samples exposed to input brine, 1976-77.

## SUMMARY

General-, pitting, and crevice-corrosion of 13 commercially available alloys were examined in seven brine and steam process environments using the high-salinity, high-enthalpy brine produced from geothermal well Magmamax No. 1 on the Salton Sea KGRA located in the Imperial Valley, Calif. Tests of 15- and 30-day durations in these environments provided a general indication of the service performance of these alloys in brines typical of the Salton Sea KGRA.

Stainless steel alloy 29-4, Inconel 625, and Hastelloys G, S, and C-276 were the most corrosion-resistant alloys in all of the process environments General corrosion rates were 0.2 mpy or less, and no pitting and little susceptibility to crevice corrosion was observed.

Stainless steel alloys type 430, E-Brite 26-1, and 6X had general corrosion rates of 2 mpy or less in all of the process environments. However, they exhibited a tendency to pit and were susceptible to crevice corrosion in some process environments.

Type 316 L stainless steel exhibited general corrosion rates of 1 mpy or less in all of the process environments but exhibited intergranular corrosion, pitted readily, and was susceptible to crevice corrosion. Pitting rates increased with time of exposure, particularly in the steam environments. In addition, transgranular cracking of 316 L stainless steel weight-loss samples due to residual stresses from cold-working occurred in all of the process environments, indicating a tendency toward stress-corrosion cracking.

TiCode-12 and titanium-1.5 nickel had general corrosion rates of 2 mpy or less in all of the process environments and did not pit. General corrosion rates appeared to increase with time of exposure. No crevice corrosion was observed with the titanium alloys.

Carbon (1020) and 4130 steels were the least resistant to general corrosion and exhibited corrosion rates up to 120 mpy. More typically, the rates ranged from 10 to 60 mpy, with the lower rates being observed for 4130 steel.

The major scale-forming mineral on the corrosion samples in all but the last two process environments (P6 and P7) was galena, with lesser amounts of other mineral species present. The porous structure of the galena deposits resulted in incomplete protection of the underlying metal from additional corrosion. It may, in fact, promote localized forms of corrosion such as pitting, crevice-, and stress-corrosion cracking, thereby rendering certain alloys more susceptible to failure.

## REFERENCES

1. Barnes, H. L., W. F. Downs, J. D. Rimstidt, and D. O. Hayba. Control of Silica Deposition in Geothermal Systems. Annual report on Bureau of Mines Grant G01551401, July 1977, 42 pp; available for consultation at Bureau of Mines Library in Avondale, Md.

2. Bird, R. B., W. E. Stewart, and E. N. Lightfoot. Transport Phenomena. John Wiley & Sons, Inc., New York, 1960, pp. 51-54.

3. Bishop, H. K. Personal communication to F. X. McCawley, June 2, 1978. Available upon request from H. K. Bishop, San Diego Gas & Electric Co., San Diego, Calif.

4. Carter, J. P., and S. D. Cramer. Corrosion Resistance of Some Commercially Available Metals and Alloys in Geothermal Brines. Ch. in Corrosion Problems in Energy Conversion and Generation, C. S. Tedmon, ed., Trans. Electrochem. Soc., 1974, p. 240.

5. Carter, J. P., and F. X. McCawley. In Situ Corrosion Tests in the Salton Sea Geothermal Brine Environments. J. Metals, v. 30, March 1978, p. 11.

6. Cramer, S. D. The Solubility of Oxygen in Geothermal Brines. Ch. in corrosion Problems in Energy Conversion and Generation, C. S. Tedman, ed., Trans. Electrochem. Soc., 1974, p. 251.

7. Cramer, S. D., and P. B. Needham, Jr. Linear Polarization Measurements at High Temperatures in Hypersaline Geothermal Brines. BuMines RI 8308, 1978 15 pp.

8. Kennan, J. H., and F. G. Keyes. Thermodynamic Properties of Steam. John Wiley & Sons, Inc., New York, 1936, p. 56.

☆U.S. GOVERNMENT PRINTING OFFICE: 1979-603-002/17

INT.-BU.OF MINES,PGH.,PA. 23729